

# Environmental Research

## Date palm responses to chronic, realistic ozone exposure in a FACE experiment --Manuscript Draft--

<b>Manuscript Number:</b>	
<b>Article Type:</b>	VSI:APPC 2021
<b>Section/Category:</b>	Environmental Chemistry and Toxicology
<b>Keywords:</b>	tropospheric ozone; date palm; volatile organic compounds; VOC; stomatal ozone flux; photosynthetic electron transport; chlorophyll a fluorescence
<b>Corresponding Author:</b>	Yasutomo Hoshika Istituto di Ricerca sugli Ecosistemi Terrestri Consiglio Nazionale delle Ricerche Sede secondaria di Firenze Sesto Fiorentino (FI), Firenze ITALY
<b>First Author:</b>	Elena Paoletti
<b>Order of Authors:</b>	Elena Paoletti Yasutomo Hoshika Leila Arab Sofia Martini Lorenzo Cotrozzi Daniel Weber Peter Ache Luisa Neri Rita Baraldi Elisa Pellegrini Heike Müller Rainer Hedrich Saleh Alfarraj Heinz Rennenberg
<b>Abstract:</b>	<p>Date palms are highly economically important species in hot arid regions, which may suffer ozone (<math>O_3</math>) pollution equivalently to heat and water stress. However, little is known about date palm sensitivity to <math>O_3</math>. Therefore, to identify their resistance mechanisms against elevated <math>O_3</math>, physiological parameters (leaf gas exchange, chlorophyll fluorescence and leaf pigments) and biomass growth responses to realistic <math>O_3</math> exposure were tested in an isoprene-emitting date palm (<i>Phoenix dactylifera</i> L. cv. Nabut Saif) by a Free-Air Controlled Exposure (FACE) facility with three levels of <math>O_3</math> (ambient [AA, 45 ppb as 24-h average], 1.5 x AA and 2 x AA). We found a reduction of photosynthesis only at 2 x AA although some foliar traits known as early indicators of <math>O_3</math> stress responded already at 1.5 x AA, such as increased dark respiration, reduced leaf pigment content, reduced maximum quantum yield of PSII, inactivation of the oxygen evolving complex of PSII and reduced performance index PI<sub>TOT</sub>. As a result, <math>O_3</math> did not affect most of the growth parameters although significant declines of root biomass occurred only at 2 x AA, suggesting that this date palm cultivar showed an intermediate susceptibility to <math>O_3</math>. The major mechanism in date palm for reducing the severity of <math>O_3</math> impacts was a restriction of stomatal <math>O_3</math> uptake due to low stomatal conductance and <math>O_3</math>-induced stomatal closure. In addition, an increased respiration in elevated <math>O_3</math> may indicate a raised capacity of catabolizing metabolites for detoxification and repair. Interestingly, date palm produced low amounts of monoterpenes, whose emission was stimulated in 2 x AA, although isoprene emission declined at both 1.5 and 2 x AA. Our results warrant more research on a biological significance of terpenoids in plant resistance against <math>O_3</math> stress.</p>

# Date palm responses to chronic, realistic ozone exposure in a FACE experiment

Elena Paoletti<sup>1</sup>, Yasutomo Hoshika<sup>1\*</sup>, Leila Arab<sup>2</sup>, Sofia Martini<sup>1</sup>, Lorenzo Cotrozzi<sup>3</sup>, Daniel Weber<sup>2,8</sup>, Peter Ache<sup>4</sup>, Luisa Neri<sup>5</sup>, Rita Baraldi<sup>5</sup>, Elisa Pellegrini<sup>3</sup>, Heike M. Müller<sup>4</sup>, Rainer Hedrich<sup>4,6</sup>, Saleh Alfarraj<sup>6</sup>, Heinz Rennenberg<sup>2,7</sup>

<sup>1</sup> IRET-CNR, Via Madonna del Piano 10, 50019 Sesto Fiorentino Firenze, Italy.

<sup>2</sup> Chair of Tree Physiology, Institute of Forest Sciences, Albert-Ludwigs-Universität Freiburg, Georges-Köhler-Allee 53, 79110 Freiburg, Germany.

<sup>3</sup> Department of Agriculture, Food and Environment, University of Pisa, Via del Borghetto 80, 56124 Pisa, Italy

<sup>4</sup> Institute for Molecular Plant Physiology and Biophysics, Biocenter, University of Würzburg, 97082 Würzburg, Germany.

<sup>5</sup> IBE-CNR, Via Piero Gobetti 101, 40129 Bologna, Italy.

<sup>6</sup> King Saud University, PO Box 2455, Riyadh 11451, Saudi Arabia.

<sup>7</sup> Center of Molecular Ecophysiology (CMEP), College of Resources and Environment, Southwest University No. 2, Tiansheng Road, Beibei District, 400715 Chongqing, P.R. China.

<sup>8</sup> Phytoprove Pflanzenanalytik, Georg-Voigt-Str. 14-16, 60325 Frankfurt am Main, Germany.

**Running head:** Date palm responses to ozone exposure

\*Corresponding author: yasutomo.hoshika(at)cnr.it

## Abstract

Date palms are highly economically important species in hot arid regions, which may suffer ozone (O<sub>3</sub>) pollution equivalently to heat and water stress. However, little is known about date palm sensitivity to O<sub>3</sub>.

26 Therefore, to identify their resistance mechanisms against elevated O<sub>3</sub>, physiological parameters (leaf gas  
1  
27 exchange, chlorophyll fluorescence and leaf pigments) and biomass growth responses to realistic O<sub>3</sub>  
2  
3  
4  
5  
28 exposure were tested in an isoprene-emitting date palm (*Phoenix dactylifera* L. cv. Nabut Saif) by a Free-Air  
6  
7  
29 Controlled Exposure (FACE) facility with three levels of O<sub>3</sub> (ambient [AA, 45 ppb as 24-h average], 1.5 x AA  
8  
9  
30 and 2 x AA). We found a reduction of photosynthesis only at 2 x AA although some foliar traits known as  
10  
11  
31 early indicators of O<sub>3</sub> stress responded already at 1.5 x AA, such as increased dark respiration, reduced leaf  
12  
13  
32 pigment content, reduced maximum quantum yield of PSII, inactivation of the oxygen evolving complex of  
14  
15  
33 PSII and reduced performance index PI<sub>TOT</sub>. As a result, O<sub>3</sub> did not affect most of the growth parameters  
16  
17  
34 although significant declines of root biomass occurred only at 2 x AA, suggesting that this date palm cultivar  
18  
19  
20  
21  
22  
23  
24  
25  
26  
27  
28  
29  
30  
31  
32  
33  
34  
35  
36  
37  
38  
39  
40  
41  
42  
43  
44  
45  
46  
47  
48  
49  
50  
51  
52  
53  
54  
55  
56  
57  
58  
59  
60  
61  
62  
63  
64  
65

**Keywords:** tropospheric ozone; date palm; volatile organic compounds; VOC; stomatal ozone flux;  
photosynthetic electron transport; chlorophyll *a* fluorescence

**Funding information:**

We are grateful for financial support to the MITIMPACT project (INTERREG V A – Italy – France ALCOTRA),  
Fondazione Cassa di Risparmio di Firenze for supporting the ozone FACE development. The authors extend  
their appreciation to the Deanship of Scientific Research at King Saud University, Saudi Arabia, for partially

50 funding this work through research group RG-1435-018. Financial support of L.A. by a short-term travelling  
1  
2 grant of the Federation of European Societies of Plant Biology (FESPB) is gratefully acknowledged.  
3

4  
5

6  
7  
8  
9

10  
11  
12  
13  
14  
15  
16  
17  
18  
19  
20  
21  
22  
23  
24  
25  
26  
27  
28  
29  
30  
31  
32  
33  
34  
35  
36  
37  
38  
39  
40  
41  
42  
43  
44  
45  
46  
47  
48  
49  
50  
51  
52  
53  
54  
55  
56  
57  
58  
59  
60  
61  
62  
63  
64  
65

53 **Introduction**

1

254

3

4

55

6

56

8

9

10

11

58

12

13

14

59

15

16

60

17

18

61

20

162

22

23

63

24

25

64

27

28

65

29

30

66

31

32

367

34

35

68

36

37

69

39

40

70

41

42

71

43

44

72

46

73

48

49

74

50

51

75

53

54

76

55

56

57

77

58

59

60

61

62

63

64

65

Surface ozone (O<sub>3</sub>) is a secondary pollutant formed via reactions from precursors, e.g. nitrogen oxides, carbon monoxide, methane and volatile organic compounds (VOC) in the presence of sunlight. It is an ubiquitous air pollutant, which at present reaches potentially phytotoxic levels in many regions of the world (Mills et al., 2018). Ozone impacts on vegetation have been largely investigated (Paoletti, 2007; Li et al., 2017; Grulke and Heath, 2020), but there is still a lack of knowledge on species from under-investigated areas of the world, e.g. on palms.

Palms are perennial flowering plants in the monocot order Arecales, mostly restricted to tropical and subtropical climates. Among the > 2600 species of palm, only date palm (*Phoenix dactylifera* L.) has been investigated for O<sub>3</sub> responses so far and showed relatively high sensitivity following short-term exposure (8 h) to a spike of O<sub>3</sub> (200 ppb) (Du et al., 2018). Date palm is appreciated both as ornamental tree and as food source, and is widely cultivated wherever the temperature is optimal for ripening of its edible sweet fruits (ab. 40 °C), especially in Northern Africa, the Middle East and South Asia. In these areas, high temperature, intense solar radiation and clear sky favour O<sub>3</sub> formation (Smoydzin et al., 2012; Radaideh, 2016). In fact, elevated O<sub>3</sub> precursor emissions and high O<sub>3</sub> pollution have been documented over the Middle East (Smoydzin et al., 2012) and South Asia (Fry et al., 2012), because of urban development and industrialization (Ohara et al., 2007; Radaideh, 2016) as well as long-range transport of precursors (Lelieveld et al., 2009; Kulshrestha and Kumar, 2014). Although date palm requires good soil water availability for optimal growth, it can tolerate drought (Arab et al., 2016). It presents thick leaves (Doaygei et al., 2013) and low gas exchanges (Arab et al., 2016) that are considered xeromorphic adaptations able to induce cross-tolerance to O<sub>3</sub> (Paoletti, 2006). Date palm sensitivity to O<sub>3</sub> is thus worth of further investigations.

78 Ozone may reduce plant growth. According to a meta-analysis by Li et al. (2017), an experimentally  
1  
279 enhanced O<sub>3</sub> exposure (mean concentrations = 116 ppb) reduced 14% of total biomass compared with the  
3  
4  
580 control (mean concentrations = 21 ppb). The negative effect was highlighted in below-ground rather than  
6  
781 above-ground growth (Agathokleous et al., 2016). A reduction in plant growth by O<sub>3</sub> is generally related to a  
8  
982 damage to photosynthetic systems in leaves (Hoshika et al., 2020a, b). Ozone-induced negative effects on  
10  
11  
1283 photosynthesis may be associated with a reduced performance of chlorophyll fluorescence and a decline of  
13  
1484 photosynthetic pigments (Li et al., 2017; Cotrozzi et al., 2018a).

15  
1685  
17  
18  
1986 Elevated O<sub>3</sub> exposure also impacts on isoprene emission from leaves. In addition to the pivotal role of VOC  
20  
2187 on O<sub>3</sub> formation in the atmosphere, biogenic isoprene biosynthesis and emission is postulated to contribute  
22  
2388 to scavenge O<sub>3</sub>-induced reactive oxygen species (ROS) (Loreto and Velikova, 2001; Vickers et al., 2009),  
24  
25  
2689 maintaining photochemical efficiency and photosynthetic stability (Pollastri et al., 2019) and acting as a  
27  
2890 signal molecule to alter gene expression for abiotic stress (Harvey and Sharkey, 2016; Zuo et al., 2019).  
29  
30  
3191 Palms usually emit isoprene from the leaves. For example, Parra (2008) and Hewitt et al. (2009) evaluated  
32  
3392 the contribution of the high-isoprene-emitting oil palm in tropical plantations to the production of surface  
34  
3593 O<sub>3</sub> pollution. Arab et al. (2016) found that heat but not drought stimulated the biosynthesis of isoprene in  
36  
37  
3894 date palm, with photosynthesis only weakly affected by both stressors.  
39

4095  
41  
4296 The aim of this study was to clarify the mechanisms of date palm sensitivity to O<sub>3</sub> exposure under realistic  
43  
44  
4597 ambient conditions in a last-generation O<sub>3</sub> Free-Air Controlled Exposure (O<sub>3</sub> FACE) experiment. The  
46  
4798 questions addressed here are: (i) does O<sub>3</sub> affect the response of biomass and leaf gas exchange  
48  
4999 (photosynthetic parameters and VOC emission) in date palm? (ii) is date palm sensitivity explained by  
50  
51  
52100 avoidance of O<sub>3</sub> stress (restriction of O<sub>3</sub> uptake due to stomatal closure)? (ii) is date palm sensitivity  
53  
54101 affected by isoprene emission from leaves?  
55

## 56 57102 58 59103 **Materials and methods**

60  
61  
62  
63  
64  
65

104  
1  
105  
3  
4  
106  
5  
6  
107  
8  
108  
10  
11  
109  
12  
13  
110  
15  
16  
111  
17  
18  
112  
19  
20  
113  
22  
23  
114  
24  
25  
115  
26  
27  
116  
28  
29  
117  
30  
31  
32  
118  
34  
35  
119  
36  
37  
120  
38  
39  
121  
40  
41  
122  
42  
43  
44  
123  
45  
46  
124  
47  
48  
125  
49  
50  
51  
126  
52  
53  
127  
54  
55  
56  
128  
57  
58  
129  
59  
60  
61  
62  
63  
64  
65

**Experimental design and conditions**

The experiment was carried out from May 20<sup>th</sup> to August 20<sup>th</sup>, 2019, in a free-air controlled exposure (FACE) facility located in Mediterranean Italy (43°48'59" N, 11°12'01" E, 55 m a.s.l.), where ambient summer conditions allow the growth of tropical plant species (Moura et al., 2018; Fernandes et al., 2019). Three levels of O<sub>3</sub> were applied: ambient (AA), 1.5 times ambient (1.5 x) and twice ambient O<sub>3</sub> concentrations (2 x), with three replicated plots per each O<sub>3</sub> level. A detailed description of the ozone FACE facility is in Paoletti et al. (2017).

Environmental conditions were continuously monitored by recording hourly values of soil moisture by ECH2O EC-5 sensors (Decagon Devices, Pullman WA, USA) and of air temperature, photosynthetic active radiation, relative humidity of the air and precipitation by a Watchdog station (Mod. 2000; Spectrum Technology, Inc., Aurora, IL, USA). Fig. 1 shows environmental conditions (Fig. 1a) and O<sub>3</sub> levels (Fig. 1b) during the experiment. AOT40 (Accumulated dose of ozone Over a Threshold of 40 ppb) values at the end of the 92 days of the experiment were 20,071 ppb·h in AA, 46,297 ppb·h in 1.5 x AA and 61,959 ppb·h in 2 x AA. POD1 (Phytotoxic Ozone Dose above a threshold of 1 nmol m<sup>-2</sup> s<sup>-1</sup>) values were 2.43 mmol m<sup>-2</sup> in AA, 3.93 mmol m<sup>-2</sup> in 1.5 x AA and 4.64 mmol m<sup>-2</sup> in 2 x AA. The details of POD1 calculation are described in Suppl. Fig. S1 and Table S1.

Forty-five micro-propagated 1-year-old plants of date palm (ab. 1 m high) of the cultivar Nabut Saif, raised in a soil-less peat-based potting mix in a plastic "torpedo" pot, were transferred into 4.5 l pots filled with 70% gravel (diameter 3-6 mm) and 30% commercial planting peat-rich soil in December 2018. Pots were kept to overwinter in a phytotron on plastic tablets continuously filled with tap water at 1-2 cm height and watered daily with 50 ml tap water per pot. Conditions included artificial illumination at ca. 200 μmol m<sup>-2</sup> s<sup>-1</sup>, 25°C temperature, with a 16/8h light/dark cycle. Plants were transferred to 20 l pots and to shaded

130 tunnels in the open on 1<sup>st</sup> May, 2019, and moved to full light after one week. Each pot was fertilized once a  
1  
131 month with NPK 20:10:20 with micronutrients (Soluplant 20.10.20, Haifa, Israel). Five potted plants were  
3  
132 placed in each plot, for a total of 45 plants. Each pot was watered daily by a drip irrigation system with 800  
5  
6  
133 ml of tap water, i.e. 90% of field capacity.  
8

134

10

11

135

### ***Measurements of gas exchange***

13

136

15

137

16

138

17

139

18

140

19

20

141

21

142

22

143

23

144

24

145

25

146

26

147

27

148

28

149

29

150

30

151

31

152

### ***Measurements of the kinetics of chlorophyll (Chl) a fluorescence***

53

153

54

154

55

155

56

57

58

59

60

61

62

63

64

65

On 20<sup>th</sup> August, Chl *a* fluorescence was measured on attached leaves dark adapted with Hansatech leaf clips (30 min) (from all the 5 plants per plot) with three leaves per plant, by a Plant Efficiency Analyser



156 (Pocket PEA fluorimeter, Hansatech Instruments Ltd., King's Lynn, UK). The emitter wavelength of a non-  
1  
157 modulated light source was 625 nm for the actinic light LED. High quality optical band pass filters were used  
3  
158 for the detector (Chl *a* fluorescence 730±15 nm). Measurements were performed on circular areas of the  
5  
159 leaves of 2 mm diameter, using Hansatech leaf clips homogeneously illuminated by actinic light LEDs set to  
8  
160 a saturating light intensity of 3500  $\mu\text{mol photons m}^{-2} \text{s}^{-1}$ . Chl *a* fluorescence was recorded within five time  
10  
161 intervals; every 10  $\mu\text{s}$  for the initial fluorescence (0 - 300  $\mu\text{s}$ ), every 100  $\mu\text{s}$  (0.3 - 3 ms), 1 ms (3 - 30 ms), 10  
12  
162 ms (0.03 - 0.3 s), 100 ms (0.3 - 1 s). Raw data were transferred and processed using PEA Plus software  
15  
163 (Hansatech Instruments Ltd.). The primary photochemistry of PSII was further evaluated using well  
17  
164 established parameters described in Suppl. Table S2, Suppl. Fig. S2 and Suppl. Fig. S3a-c, according to  
20  
165 formulations previously published (Papageorgiou and Govindjee, 2004; Strasser et al., 2010; Bussotti et al.,  
22  
166 2011; Chen et al., 2016). The changes in these parameters are associated with various stressors as well as  
24  
167 overall plant vitality (Kalaji et al., 2017). All parameters were optimized for a high throughput workflow of  
27  
168 Chl *a* fluorescence raw data using the open source software "Libre Office 6" (The Document Foundation,  
29  
169 Berlin, Germany). The data were plotted graphically and statistically analyzed by using "Prism 8.4 for Mac  
31  
170 OS-X" software (GraphPad Software Inc., La Jolla, USA).

### 171 172 ***Measurement of synthesis and emission of volatile organic compounds***

173  
174 On August 1<sup>st</sup>-2<sup>nd</sup>, from 10 to 12 CET, one leaf (2<sup>nd</sup> fully expanded leaves) from two plants per replicated  
43  
175 plot was sampled for emission of VOC following the methodology by Yuan et al. (2016). In detail, the  
46  
176 central part of the leaf was included into the 6 cm<sup>2</sup> cuvette of a LI-6400 system (Li-Cor 6400 instruments,  
48  
177 Lincoln, NE, USA). Measurements were performed at standard conditions of 30°C and 1000  $\mu\text{mol m}^{-2} \text{s}^{-1}$   
50  
178 PPF. When photosynthesis reached a steady state, 2-l air samples were collected through a purified  
53  
179 Tenax-TA glass tube (Thermal Desorption Tubes, filled with 100 mg Tenax-TA adsorbent (Mesh 60/80),  
55  
180 Gerstel, Germany) with a vacuum sampler pump (VSS-1, AP Buck, USA). Blank (no leaf) samples were  
58  
181 collected at the beginning and end of each day of sampling. The traps were sealed with Teflon-coated brass  
60  
61  
62  
63  
64  
65

182 caps immediately after collection and stored at -20°C until analysis to avoid any chemical alteration and/or  
1  
183 artefacts. Then, the samples were processed and analyzed with a thermal-desorber (Markes International,  
3  
184 Series 2 Unity) connected to a 7890 A gas chromatograph coupled with a 5975C mass detector (GC-MS,  
5  
6  
185 Agilent Technologies, Wilmington, USA) as described in Baraldi et al. (2019). Identification and  
8  
186 quantification of the sampled isoprenoids were carried out according to Rapparini et al. (2004).  
10

11  
187  
12  
13  
188 All pinnae of the 2<sup>nd</sup> fully expanded leaf of each plant were cut into small pieces, shock frozen in liquid  
15  
189 nitrogen and ground to fine powder. RNA was isolated using the NucleoSpin RNA Plant Kit (Macherey-  
17  
190 Nagel) according to the manufacturers advice with the following exceptions. Leaf tissues were frozen in  
20  
191 liquid nitrogen and ground to powder. For each sample, 50 mg of leaf tissue powder were first mixed with  
22  
192 500 µl Fruit-mate™ (Taraka Bio Inc.) and centrifuged for 5 min at 4 °C and 12000 g to remove  
24  
25  
193 polysaccharides and polyphenols. The supernatant was mixed with 500 µl RA1 buffer (containing 1:1000  
27  
194 TCEP) from the NucleoSpin RNA Plant Kit. The mixture was transferred to the filter columns in two steps  
29  
195 and the filtrate was collected in a new collection tube and mixed well with the same volume of 70%  
31  
32  
196 ethanol. The mixture was added again in two steps to the NucleoSpin RNA plant Colum and centrifuged for  
34  
35  
197 1 min at 11,000 g. The washing steps were performed following the manufacturer's instructions. RNA was  
36  
37  
198 eluted in 33 µL RNase free water that was incubated twice on the membrane for 1 min. The concentration  
39  
40  
199 was determined using a Nanodrop ND-1000 spectrophotometer (Thermo Fisher Scientific, Wilmington, DE,  
41  
42  
200 U.S.A.). Removal of contaminating DNA, cDNA synthesis and qPCR was performed as described previously  
43  
44  
201 (Böhm et al., 2018). The following primers were used for qPCR and transcript numbers were normalized to  
46  
47  
202 10,000 transcripts of the housekeeping gene, the growth elongation factor EF1a (Patankar et al., 2016):  
48  
49  
203 PdEF1afwd (5'-CTGTTGCAACAAGATGGA-3'), PdEF1arev (5'-CCGAAGGTGACAACCATA-3'), Pd\_ISPSfwd (5'-  
50  
51  
204 CGTCCTATTAGTCCATGCT-3'), Pd\_ISPSrev (5'-GATGGATGTTGGAGTATC-3'), PdMTPS1fwd (5'-  
53  
54  
205 TTCCAAGAATCATAAAGGCTA-3'), PdMTPS1rev (5'-AGTCATATTAAGACTC-3'), Pd-LevSynfwd (5'-  
55  
56  
206 TGCCTCCCATATTCAAGCAT-3'), Pd-LevSynrev (5'-AGGTACATGAAGCGTGAG-3'), where PdEF1 is growth  
57  
58  
207 elongation factor EF1a (NCBI accession XM\_008785500.3), Pd\_ISPS is a putative isoprene synthase (NCBI  
60  
61  
62  
63  
64  
65

208 accession XM\_008781287.2) and Pd\_MTPS1 is a putative monoterpene synthase (NCBI accession  
1  
209 XM\_026807289.1). Pd\_ISPS primers were designed for the putative date palm isoprene synthase  
3  
4  
210 (TRINITY\_GG\_87144\_c19\_g1\_i1.p1 from Helmholtz II experiment, unpublished). ISPS transcripts were  
5  
6  
211 normalized to 10000 molecules of HKG EF1 $\alpha$  using standard curves calculated for individual PCR products.  
8

212

10

11

213 **Measurement of foliar traits and pigments**

12

13

214

15

215 After the leaf gas exchange measurements, five leaf discs of 0.8 cm diameter per the same target leaf (one  
17

18

216 leaf, 2<sup>nd</sup> fully expanded leaves, one to two plants per plot) were collected by using a leaf punch (Fujiwara  
20

217 Scientific Company Co., Ltd., Tokyo, Japan), and weighted by a scale (Model Bp110, Sartorius weighing  
22

23

218 technology, Germany) in order to calculate fresh weight of the samples (FW). They were then dried at 70°C  
24

25

219 for at least 72 h in the oven. Leaf mass per area (LMA) was calculated as a ratio of dry mass (DW) and area  
27

220 (LA) of each leaf. Leaf water content was calculated as  $LWC (\%) = (FW - DW) / FW \times 100$ .  
29

30

221

31

32

222 Other leaf samples (ca. 3 g) of each target leaf (one leaf, 2<sup>nd</sup> fully expanded leaves, one plant per plot) were  
34

223 harvested, immediately flash-frozen with liquid nitrogen and stored at -80°C until leaf pigment analysis.  
36

37

224 Leaf pigments were determined by ultra high performance liquid chromatography (UHPLC) using a Dionex  
39

40

225 UltiMate 3000 system equipped with an Acclaim 120 C18 column (5- $\mu$ m particle size, 4.6-mm internal  
41

226 diameter  $\times$  150-mm length) maintained into a Dionex TCC-100 column oven at 30 °C, and a Dionex UVD  
43

44

227 170U detector (Thermo Scientific, Waltham MA, USA; Cotrozzi et al., 2018b). Leaf material (50 mg fresh  
46

228 weight, FW) was homogenized in 1 mL of 100% HPLC-grade methanol and incubated overnight at 5 °C in  
48

229 the dark. The sample supernatants were filtered through 0.2  $\mu$ m Minisart® SRT 15 aseptic filters. The  
50

51

230 pigments were eluted using 100% solvent A (acetonitrile/methanol, 75/25, v/v) for the first 14 min to elute  
53

231 xanthophylls (neoxanthin, Neo; violaxanthin, Vio; antheraxanthin, Ant; lutein, Lut; zeaxanthin, Zea; in order  
55

232 of elution), followed by a 1.5-min linear gradient to 100% solvent B (methanol/ethylacetate, 68/32, v/v),  
56

233 which was pumped for 14.5 min to elute chlorophyll b (Chl b) and chlorophyll a (Chl a) and  $\beta$ -carotene ( $\beta$ -  
60

61

62

63

64

65

234 car), followed by 2-min linear gradient to 100% solvent A. The flow rate was 1 ml min<sup>-1</sup>. The column was  
1  
235 allowed to re-equilibrate in 100% solvent A for 1 min before the next injection. The pigments were  
3  
236 detected by their absorbance at 445 nm. To quantify the pigment content, known amounts of pure  
4  
5  
6  
237 standards were injected into the UHPLC system and an equation correlating the peak area to pigment  
8  
238 concentration was formulated. The data were processed using the Thermo Scientific Dionex Chromeleon 7  
10  
11  
239 Chromatography Data System software. Total chlorophyll content (Chl<sub>TOT</sub>) was calculated as Chl a + Chl b.  
12  
13  
240 Total carotenoid content (Car<sub>TOT</sub>) was calculated as Neo + Vio + Ant + Lut + Zea + β-car, while the  
15  
16  
241 xanthophyll cycle pigment content (VAZ) was calculated as Vaz + Ant + Zea. The de-epoxidation state (DEPS)  
17  
18  
242 was calculated as (Ant + Zea)/VAZ.  
20  
21  
243

#### 244 ***Assessment of growth and biomass***

245  
27  
246 Plant height, number of leaves and base diameter were recorded at the beginning and the end of the  
29  
30  
247 experiment with a ruler and a caliper with 1-mm accuracy. Total above- and below-ground biomass of all  
31  
32  
248 plants was harvested at the end of the experiment and put in the oven at 70 °C until constant weight was  
34  
35  
249 reached (ab. 72 hours). After that, DW of each plant organ was determined by a scale (Model Bp110,  
36  
37  
250 Sartorius weighing technology, Germany).  
38  
39

#### 40 41 42 ***Statistical analysis***

43  
44  
45  
46  
47  
254 Data from the plants in each plot were averaged and the average was used as statistical unit, i.e. N = 3  
48  
49  
255 plots. Data were tested for normal distribution and homogeneity of variance by Smirnov and Levene tests,  
50  
51  
256 respectively. The effects of O<sub>3</sub> on the linear relationship between g<sub>s</sub> and VPD were tested by an analysis of  
53  
54  
257 covariance (ANCOVA). To assess the effect of O<sub>3</sub> and measurement time on A and g<sub>s</sub>, we applied a two-way  
55  
56  
258 analysis of variance (ANOVA). For the other parameters, the effect of O<sub>3</sub> was tested by one-way ANOVA  
58  
59  
60  
61  
62  
63  
64  
65

259 followed by Tukey's multiple comparison test. All statistical tests were carried out by R software (R 3.5.1: R  
1  
260 Core Team, 2018).

261

## 262 Results

263

264

### 264 *Foliar traits and pigments*

265

266

266 Date palms showed LMA values in the range of 119 to 133 g m<sup>-2</sup> (Tab. 1). There were no significant effects

267

268

269

270

271

272

273

274

275

276

277

278

279

280

281

282

283

284

285

286

287

288

289

290

291

292

293

294

295

296

297

of O<sub>3</sub> on LMA, while LWC was increased by O<sub>3</sub>. In fact, LWC values were significantly higher in 2 × AA than in AA plants (+19%).

Contents of Chl<sub>TOT</sub> and Car<sub>TOT</sub> significantly decreased only under 1.5 × AA, compared with AA (-22 and -32%, respectively), while VAZ decreased under both 1.5 × AA and 2 × AA (ca. -30%; Tab. 1). Lut values were 26% lower under 1.5 x AA than under 2 x AA, but there were no significant difference comparing these enriched O<sub>3</sub> concentrations with AA. No significant O<sub>3</sub> effects were found on Chl a/b ratio, β-car, and DEPS.

### 275 *Leaf gas exchange*

276

277

278

279

280

281

282

283

284

285

286

287

288

289

290

291

292

293

The daily measurements of leaf gas exchange indicate a significant effect of O<sub>3</sub> on A and g<sub>s</sub> (Tab. 2). Only the highest 2 × AA O<sub>3</sub> treatment induced a significant decline of A (-51% on July 23<sup>rd</sup> and -48% on July 30<sup>th</sup>) and g<sub>s</sub> (-57% on July 23<sup>rd</sup> and -59% on July 30<sup>th</sup>) relative to AA, which occurred only in the morning, although the interaction of daytime and O<sub>3</sub> treatment was not significant. The responses of g<sub>s</sub> to VPD are shown in Fig. 2. Stomatal conductance decreased with increasing VPD at AA and 1.5 x AA treatments. An ANCOVA test revealed that the y-intercept of the relationship between g<sub>s</sub> and VPD was lower in 1.5 x AA compared to the control (AA). There was no statistically significant relationship between g<sub>s</sub> and VPD at the highest

284 level of O<sub>3</sub> treatment (2.0 x AA). Dark respiration rate (R<sub>n</sub>) was significantly lower in AA than in 1.5 AA and 2  
1  
285 x AA plants (-28% and -36%, respectively) (Fig. 3).

286  
287 Parameters of the stomatal conductance model are shown in Table S1 and Fig. S1. The maximum stomatal  
288 conductance to O<sub>3</sub> (g<sub>max</sub>) value was set to 73 mmol O<sub>3</sub> m<sup>-2</sup> PLA s<sup>-1</sup> as 95<sup>th</sup> percentile of g<sub>sto</sub> measurements  
289 (Table S1, Fig. S1). The minimum stomatal conductance (f<sub>min</sub>) value was set to 0.06 (fraction) corresponding  
290 to the 5<sup>th</sup> percentile values of the stomatal conductance recorded throughout the measurements. Stomatal  
291 response to light (f<sub>light</sub>) showed a typical saturation curve with a light saturation point above 2000 μmol m<sup>-2</sup>  
292 s<sup>-1</sup> (Fig. S1a). The f<sub>O<sub>3</sub></sub> indicates that O<sub>3</sub> decreased stomatal conductance by 0.31% per unit O<sub>3</sub> concentration  
293 (ppb) in date palm leaves (Fig. S1b). The optimal temperature for stomatal opening was 27 °C (Fig. S1c).  
294 VPD higher than 2.6 kPa induced stomatal closure (Fig. S1d).

### 296 **Chlorophyll *a* fluorescence**

297  
298 At ambient O<sub>3</sub> level, the induction curve was significantly higher than in the palm leaves exposed to  
299 elevated O<sub>3</sub> levels after 300 μs (Fig. S2). The curves of leaves exposed to 1.5 x AA and 2 x AA O<sub>3</sub> exposure  
300 exhibited a similar pattern. The relative variable fluorescence ΔV showed marked differences between the  
301 AA controls and the two elevated O<sub>3</sub> treatments (Fig. S3a), with the biggest differences within the O-J-  
302 phase and the J-I-phase and a lower difference within the I-P-phase, but without a distinct peak at the J-  
303 Step and the I-Step (marked as ΔV<sub>J</sub> and ΔV<sub>I</sub>). This presentation of fluorescence kinetics showed only a small  
304 difference between both groups of O<sub>3</sub> treated leaves at 150 μs compared to the AA group (Fig. S3b). On the  
305 other hand, marked differences between the control group at ambient O<sub>3</sub> and the two groups exposed to  
306 1.5 and 2 times enhanced O<sub>3</sub> concentrations were identified in ΔW<sub>O<sub>3</sub></sub> (Fig. S3c) with a peak marked as ΔW<sub>K</sub>  
307 at an average time of 500 μs. At the beginning of the fluorescence kinetics after 150 μs of illumination,  
308 values at the L-Step were similar between AA and O<sub>3</sub> treatments (Fig. 4a). In addition, marked differences in  
309 the extent and range of the resulting values at the K-Step (t = 300 to 600 μs) were observed between O<sub>3</sub>

310 treatments and AA, with mostly positive values indicating that the fluorescence level of O<sub>3</sub> treated date  
1  
311 palm leaves at this step was higher than in AA (Fig. 4b). The variable fluorescence levels at step J (t = 2 ms)  
3  
312 and I (t = 30 ms) also showed marked differences between O<sub>3</sub> treated plants and the AA group (Fig. 4c,d).  
5  
6

313  
8

314 The quantum yield of photosystem II ( $\phi_{Po}$ ) showed statistically significant differences between AA and  
10  
315 leaves of plants growing at 1.5 x AA and 2 x AA, but no differences were found between 1.5 x AA and 2 x AA  
12  
316 (Fig. 5a). The same findings were observed for the performance index PI total (Fig. 5b) and for the number  
15  
317 of reaction centers per absorption (10RC/ABS, Fig. 5d). One-way ANOVA revealed a significant difference ( $p$   
17  
318 < 0.05) between AA and 1.5 x AA for the energy dissipation per active reaction center chlorophyll DI<sub>0</sub>/RC  
20  
319 (Fig. 5c). However, there were no statistically significant differences between AA and 2 x AA as well as  
22  
320 between 1.5 x AA and 2 x AA for this parameter.  
24  
25

321  
27

### 322 **Volatile organic compounds**

29

30  
323  
31

324 Isoprene emission was significantly impaired by both elevated O<sub>3</sub> treatments (-58% at 1.5 x AA and -50% at  
34  
325 2 x AA), while the relative expression of isoprene synthase transcripts showed a large variability and no  
36  
326 clear response to O<sub>3</sub> (Fig. 6a,b). Date palm emitted also small amounts of monoterpenes such as  $\alpha$ -pinene,  
39  
40  
327  $\beta$ -pinene, octanal, nonanal, camphor, iso-borneol (data not shown), whose emission was stimulated in 2 x  
41  
328 AA plants, so that the emission of total VOCs decreased only at 1.5 x AA (-57% relative to AA) (Fig. 6c,e).  
44  
329 Also the relative expression of monoterpene synthases was very variable and the increases at 2 x AA were  
46  
330 not statistically significant (Fig. 6d). Isoprene emission was correlated positively with net photosynthesis  
48  
331 (Fig. 7a) and negatively with intercellular CO<sub>2</sub> concentration (C<sub>i</sub>) (Fig. 7b). However, such correlations were  
51  
332 not found in monoterpene emission.  
53

54  
333  
55

### 334 **Growth and biomass**

58

59  
335  
60

61  
62  
63  
64  
65

336 Plant height, number of leaves and base diameter were not affected by O<sub>3</sub> treatments (data not shown).  
1  
337 However, during the 3-month experiment, the plants significantly increased in diameter from the beginning  
3  
338 of the experiment (2.06 ± 0.31 cm) to the end (2.80 ± 0.46 cm), while plant height (107 ± 8.9 cm vs. 111 ±  
5  
339 9.4 cm) and number of leaves (5.5 ± 1.0 vs. 6.0 ± 0.8) were unaltered. Above- and below-ground biomass  
8  
340 decreased with increasing O<sub>3</sub> treatments, but the effect was significant only for the 2 x AA roots relative to  
10  
341 AA roots (-36%) (Fig. 8a,b).  
12

1342

## 343 Discussion

1344

345 The growth conditions at the study site were suitable for date palm as suggested by the increase in base  
22  
346 diameter over the experiment. For instance, the average diurnal air temperature was 19.5/27.8/29.2/30.1  
24  
347 °C in May/June/July/August, i.e. in the range of values in Riyadh, Saudi Arabia (31.1/33.7/34.8/32.7 °C), that  
27  
348 is one of the major area of date palm distribution and cultivation (Aleid et al., 2015). The stomatal  
29  
349 conductance model showed that the optimal temperature for stomatal opening was 27 °C in this date palm  
31  
350 cultivar. The O<sub>3</sub> levels were realistic as they well simulated the conditions in Riyadh. For instance, the O<sub>3</sub>  
34  
351 peaks in May/June/July/August were 72/110/105/92 ppb at the ozone FACE and 66/95/98/90 ppb in  
36  
352 Riyadh (Butenhof et al., 2015). Such realistic O<sub>3</sub> levels translated into very high values of AOT40. At the end  
38  
353 of the experiment, in fact, the date palms were exposed to AOT40 levels that were 4 (AA), 9.2 (1.5 x AA)  
41  
354 and 12.4 (2 x AA) times higher than the critical level recommended to protect plants from O<sub>3</sub> injury, i.e. 5  
43  
355 ppm h (CLRTAP, 2014).  
46

356

### 357 *Photosynthetic responses to ozone exposure*

358

359 Elevated O<sub>3</sub> exposure induced significant negative effects on date palm photosynthesis in the morning,  
55  
360 especially at the highest 2 x AA O<sub>3</sub> level. Stomatal resistance to CO<sub>2</sub> transport may be considered as a factor  
58  
361 to limit photosynthetic activity in elevated O<sub>3</sub> (Kitao et al., 2009; Hoshika et al., 2020b). In fact, stomatal  
60



362 closure due to elevated O<sub>3</sub> exposure was observed in the morning for date palm plants. However, such  
1  
363 stomatal closure cannot be found in the afternoon, suggesting that the closing response induced by  
3  
364 atmospheric humidity deficit may over-rule stomatal sensitivity to O<sub>3</sub>. Interestingly, the highest O<sub>3</sub>  
4  
5  
6  
365 treatment (2 x AA) induced a loss of stomatal response to VPD. It has been shown that O<sub>3</sub> exposure causes  
8  
366 an impairment of efficient stomatal control of gas exchange, i.e. stomatal sluggishness (Paoletti, 2005;  
10  
367 Hoshika et al., 2019, 2020a). Hoshika et al. (2019) demonstrated that the sluggish response of stomata was  
11  
12  
13  
368 attributed to ethylene emission. However, the mechanisms are still under investigated.

15  
16  
369  
17  
18  
370 A reduction of photosynthesis due to elevated O<sub>3</sub> exposure may be caused by not only stomatal but also  
19  
20  
371 biochemical limitation (Hoshika et al., 2020b). In fact, an impairment of the gas exchange was in  
21  
22  
372 accordance with the overall reduction of photosynthetic pigments (i.e. Chl<sub>TOT</sub> and Car<sub>TOT</sub>) which play a  
23  
24  
25  
373 crucial role in light harvesting for photosynthesis. The degradation of chlorophyll and carotenoids was  
26  
27  
374 similarly found in O<sub>3</sub> exposed leaves due to oxidative-stress destruction (Watanabe et al., 2013; Cotrozzi et  
28  
29  
30  
375 al., 2018a). Fast chlorophyll fluorescence kinetics of dark-adapted samples indicated that O<sub>3</sub> exposure  
31  
32  
376 strongly affected photosynthetic electron transport in date palm leaves. Ozone exposure decreased the  
33  
34  
377 maximum quantum efficiency of PSII ( $\phi_{PO}$ ;  $F_V/F_M$ ), the average performance ( $PI_{TOT}$ ), and the activity of PSII  
35  
36  
37  
378 RCs as reported before (Contran et al., 2009; Bussotti et al., 2011; Pellegrini et al., 2011; Salvatori et al.,  
38  
39  
40  
379 2013; Zhang et al., 2018b). Recently, we developed a new spectroscopic model to predict these  
41  
42  
380 fluorescence parameters in date palm (Cotrozzi et al., 2020). For a detailed analysis of hyperspectral  
43  
44  
381 parameters *see* Cotrozzi et al. (2020). In addition, our results show clear differences within the OJ-phase  
45  
46  
47  
382 between the control AA group and the two groups growing at elevated O<sub>3</sub>. The differences in the  
48  
49  
383 functionality of PSII of date palms exposed to elevated O<sub>3</sub> were not caused by a lesser connectivity between  
50  
51  
384 PSII units, since there was no significant difference of the fast fluorescence kinetics at 150  $\mu$ s between  
52  
53  
385 plants exposed to either elevated O<sub>3</sub> treatment or AA. Many studies demonstrated that inactivation of the  
54  
55  
386 oxygen evolving complex (OEC) is a typical reaction of plants to abiotic stress like heat stress or drought  
56  
57  
387 (Oukarroum et al., 2007; Oukarroum et al., 2009; Hu et al., 2020). This inactivation leads to an inhibition of  
58  
59  
60  
61  
62  
63  
64  
65

388 electron transport by releasing the manganese cluster, the main component of OEC, thereby causing an  
1  
389 imbalance between the electron flow from the OEC to the RCs (Chen et al., 2016). Studies on the effect of  
3  
390 elevated O<sub>3</sub> on the photosynthetic performance of several woody species such as beech, oak and poplars  
5  
391 showed that inactivation or breakdown of OECs represent an early response to O<sub>3</sub> stress (Bussotti et al.,  
8  
392 2011; Desotgiu et al., 2013), as also observed in our experiment.

11  
393  
13  
394 Differences were not only found within the OJ-phase, but also the JI-phase and to a lesser extent the IP-  
15  
395 phase. The JI-phase is related to the redox state of the plastoquinone pool (Tóth et al., 2007). Its redox is  
17  
396 affected by oxidative stress caused by O<sub>3</sub>, probably via the plastidic NADH-plastoquinone oxidoreductase  
20  
397 (Ndh) complex (Guéra et al., 2005). Thus, the present findings suggest that oxidative stress due to O<sub>3</sub>  
22  
398 exposure led to disturbances in the plastoquinone pool of the photosynthetic electron transport chain. The  
24  
399 IP-phase of the fluorescence transient is related to photosystem-I (PSI) activity (Schansker et al. 2005),  
27  
400 indicates the rate of reduction of ferredoxin (Cascio et al., 2010) and is thought to constitute a measure of  
29  
401 PSI electron acceptors (Tsimilli-Michael and Strasser, 2008; Živčák et al., 2014). Experiments with *Quercus*  
31  
402 *ilex* L. and *Arbutus unedo* L. showed that the activity of PSI has a key role in O<sub>3</sub>-mediated oxidative stress  
34  
403 (Mereu et al., 2011). Bussotti et al. (2011) reported that the main impact of O<sub>3</sub>-mediated oxidative stress  
36  
404 was in and beyond PSI for poplar hybrids. However, our results suggest that date palms were less sensitive  
39  
405 to O<sub>3</sub> in the last part of the photosynthetic electron transport chain, with only a minor effect on PSI activity.

41  
42  
406  
43

#### 407 *Isoprene and monoterpene responses to ozone exposure*

46  
408  
48  
49  
409 Volatile isoprenoids such as isoprene and monoterpenes are among the most abundant and reactive  
50  
51  
52 biogenic VOCs produced by plants (Guenther et al., 2012). Isoprene-emitting species occur in many plant  
53  
54 taxa across many functional types, but they are more often found in woody plant species including palms  
55  
56 (Kesselmeier and Staudt, 1999). Our date palms emitted low amounts of isoprene (on average  $8.4 \pm 0.8$  ng  
57  
58 m<sup>-2</sup> s<sup>-1</sup> in AA) relative to literature data for this species ( $\sim 27$  ng m<sup>-2</sup> s<sup>-1</sup> in Arab et al., 2016, still at 30 °C but  
59  
60  
61  
62  
63  
64  
65

414 under 1200  $\mu\text{mol m}^{-2} \text{s}^{-1}$  PAR). Tree species on average emit 22-79  $\text{ng m}^{-2} \text{s}^{-1}$  isoprene at or near standard  
1  
415 conditions, but different leaf environments and measurement techniques may significant affect such values  
3  
416 (Geron et al., 2001). Isoprene emission from date palm leaves declined at both 1.5 and 2 x AA relative to  
5  
6  
417 AA, while the relative expression of isoprene synthase transcripts did not respond to  $\text{O}_3$ . Photosynthesis  
8  
418 and isoprene emission declined in tandem, which is supported by a meta-analysis of isoprenoid responses  
10  
419 to abiotic factors including  $\text{O}_3$  (Feng et al., 2019).  
12

13  
420  
15  
421 Interestingly, date palm also produced low amounts of total monoterpenes (on average  $1.8 \pm 0.3 \text{ ng m}^{-2} \text{ s}^{-1}$   
17  
422 in AA), whose emission was stimulated in 2 x AA leaves, although an increase in the relative expression of  
20  
423 monoterpene synthase transcripts in 2 x AA leaves was not statistically significant. The stimulation of  
22  
424 monoterpene emission by  $\text{O}_3$  exposure was similarly reported mainly in evergreen species by the meta-  
24  
425 analysis (Feng et al., 2019). The monoterpene emission from date palm leaves in elevated  $\text{O}_3$  was not  
27  
426 dependent on photosynthesis. The uncoupling of monoterpene emission from photosynthesis may be a  
29  
427 hormetic response to the initial stage of stress (Agathokleous et al., 2018).  
31

32  
428  
34  
429 *Biomass responses to ozone exposure*  
36

37  
430  
39  
431 A leaf-level photosynthetic activity may be closely related to plant growth. As a result of  $\text{O}_3$ -induced  
41  
432 damage to photosynthetic activity, biomass accumulations are usually limited (Li et al., 2017; Gao et al.,  
43  
433 2017). In date palm, however, plant height, number of leaves, base diameter and above-ground biomass  
46  
434 were not significantly affected by elevated  $\text{O}_3$  exposure, while root biomass was reduced only at the  
48  
435 highest 2 x AA level. It is well known that a reduction of photosynthate allocation to roots is one of the first  
50  
51  
436 steps of  $\text{O}_3$  injury to plants (Carriero et al., 2015; Mrak et al., 2019). Decrease in root biomass due to  $\text{O}_3$  was  
53  
437 reported in approx. 40% of studies on trees according to a meta-analytic review (Agathokleous et al., 2016).  
55

56  
438  
58  
439 *Reasons of intermediate susceptibility to ozone*  
60

440  
1  
441  
3  
442  
5  
6  
443  
8  
444  
10  
445  
12  
446  
15  
447  
17  
448  
20  
449  
22  
450  
24  
451  
27  
452  
29  
453  
31  
454  
34  
455  
36  
456  
39  
457  
41  
458  
43  
459  
46  
460  
48  
461  
50  
462  
53  
463  
55  
464  
57  
58  
59  
60  
61  
62  
63  
64  
65

Ozone exposure did not significantly affect most of the growth parameters, although 2 x AA O<sub>3</sub> exposure reduced below-ground biomass. These results indicate that this date palm cultivar may be intermediately susceptible to O<sub>3</sub>. In fact, evergreen species such as date palm is more resistant to O<sub>3</sub> than deciduous species (Feng et al., 2018), because larger availability of cell walls implies larger apoplastic substrate for O<sub>3</sub> detoxification (Moldau, 1998). However, plant resistance to O<sub>3</sub> may depend not only on leaf habit (deciduous and evergreen) but also various physiological factors (Feng et al., 2018).

A well-known factor mitigating O<sub>3</sub> susceptibility of plant species is low stomatal conductance and, thus, restricted stomatal O<sub>3</sub> uptake (Reich, 1987). Here we present a Jarvis-type stomatal conductance model for estimating the maximum g<sub>s</sub> in this species and estimated a g<sub>max</sub> value (73 mmol O<sub>3</sub> m<sup>-2</sup> s<sup>-1</sup>) that is in line with the values of desert shrubs and in the lower range of global values found in a meta-analysis of g<sub>s</sub> in woody plants (Hoshika et al., 2018). Although our g<sub>max</sub> value was slightly higher than previous observations of g<sub>s</sub> in the same species (40 to 50 mmol O<sub>3</sub> m<sup>-2</sup> s<sup>-1</sup>, Du et al., 2018; Kruse et al., 2017, 2019), a previous Jarvis-type g<sub>s</sub> modeling study on *P. dactylifera* found a much higher g<sub>max</sub> in a different cultivar (ab. 200 mmol O<sub>3</sub> m<sup>-2</sup> s<sup>-1</sup> in cv. Medjool, Sperling et al 2014). Stomatal conductance of different date palm cultivars may differ considerably (Al-Jabr et al., 2007), thus suggesting that further cultivar-specific studies are also needed. Such a low capacity of stomatal O<sub>3</sub> uptake implied an uncoupling of AOT40 and POD1 values. In fact, AOT40 values at the end of the experiment were 2.3 and 3.1 times higher than AA, while POD1 values were only 1.6 and 1.9 times higher in 1.5 x AA and 2 x AA, respectively, which well synthesizes the elevated stomatal defense capacity of date palm from elevated atmospheric concentrations of O<sub>3</sub>. As a matter of fact, the function f<sub>O<sub>3</sub></sub> indicates that O<sub>3</sub> decreased stomatal conductance by 0.31% per unit O<sub>3</sub> concentration (ppb) in date palm. As a result, 2 x AA O<sub>3</sub> exposure reduced g<sub>s</sub> by 46%. Ozone-induced stomatal closure may act as an avoidance response to reduce a possible O<sub>3</sub> damage to plants (Hoshika et al., 2020a).

465 Stomatal closure, however, may also cause excess light energy and production of reactive oxygen species  
1  
466 (ROS), which raises susceptibility to photoinhibitory damage (Takagi et al., 2017; Giudi et al., 2019). It  
3  
467 seems that date palm plants adopted a major protective mechanism to reduce the absorption of excitation  
4  
5  
6  
468 energy and preserve photosystems from photoinhibition through a reduction in the number of light-  
8  
469 harvesting antennae rather than in the chlorophyll antenna size (as confirmed by the unchanged values of  
10  
11  
470 Chl a/b ratio; Cotrozzi et al., 2018b). Indeed, no other differential responses in leaf pigment parameters  
12  
13  
471 were observed between plants exposed to 1.5 and 2 x AA levels. Although a reduction of VAZ was  
15  
16  
472 observed, other well-known photo-protective mechanisms (i.e. changing chlorophyll composition,  
17  
18  
473 increasing  $\beta$ -car levels and DEPS; Esteban et al., 2015) were not activated, indicating that a re-organization  
20  
21  
474 of the photosynthetic apparatus did not occur and confirming the intermediate susceptibility to O<sub>3</sub> of date  
22  
23  
475 palm.  
24

25  
26  
27  
477 The ability of increasing dark respiration under O<sub>3</sub> stress may have also contributed to mitigate the  
29  
30  
478 susceptibility of date palm. While the respiratory CO<sub>2</sub> loss is a major cause for the reduction of carbon gain  
31  
32  
479 due to elevated O<sub>3</sub> (Zhang et al., 2018a; Podda et al., 2019), dark respiration is important in the  
34  
35  
480 biosynthetic processes of growth and maintenance, which raises a metabolic capacity for repair of  
36  
37  
481 damaged tissues and detoxification especially under abiotic and/or biotic stress (Weraduwege et al., 2011).  
38  
39  
482 In fact, no oxidative damage (assessed in terms of lipid peroxidation) was observed under both increased  
41  
42  
483 O<sub>3</sub> concentrations, with a slight decrease of hydrogen peroxide reported only under 2 x AA (Arab et al. in  
43  
44  
484 prep). This response was due to an ability of date palm to regulate its major enzymatic and non-enzymatic  
46  
47  
485 antioxidants. In particular, the decreased Car<sub>tot</sub> (only under 1.5 x AA) and VAZ values indicate that these  
48  
49  
486 compounds could be consumed by the cell in order to counteract the possible reactive oxygen species  
50  
51  
487 generation by preventing their peroxidation action. Is it known that they are involved in non-photochemical  
53  
54  
488 quenching mechanisms, thus reducing the risk of photo-oxidative stress (Niinemets et al., 2003). Based on  
55  
56  
489 relative physical-chemical features and intra-cellular distribution, these antioxidant compounds may serve  
57  
58  
490 distinct and complementary functions (Close and Beadle, 2003).  
60  
61  
62  
63  
64  
65

491  
1  
492  
3  
493  
5  
6  
494  
8  
495  
10  
496  
12  
497  
15  
498  
17  
499  
20  
500  
22  
501  
24  
502  
27  
503  
29  
504  
31  
505  
34  
506  
36  
507  
39  
508  
41  
509  
43  
510  
46  
511  
48  
512  
50  
513  
53  
514  
55  
515  
58  
516  
60  
61  
62  
63  
64  
65

If isoprene emission confers protection to date palm against O<sub>3</sub> injury (Loreto and Velikova, 2001; Velikova et al., 2005), we may expect that synthesis and emission of isoprene increased with increasing O<sub>3</sub> exposure. However, our results contrasted with this hypothesis, suggesting that isoprene emission from date palm leaves may have not contributed to the protection against O<sub>3</sub> stress. A recent review questioned the common belief that isoprene has immediate, physical effects on plants such as changing membrane properties or quenching ROS (Lantz et al., 2019), because it is highly volatile and does not dissolve into cellular components in great quantity (Harvey et al., 2015). Interestingly, on the other hand, O<sub>3</sub> increased monoterpene emission, which may be also considered as a factor to protect plants from O<sub>3</sub> damage (Fares et al., 2008). While isoprene and monoterpenes share common biosynthetic pathways, monoterpenes are usually stored after synthesis in special organs, such as resin ducts or glands (Kesselmeier and Staudt, 1999). So far, it is unclear whether O<sub>3</sub> may have a direct effect on the storage pools of monoterpenes, and also the number of O<sub>3</sub> studies on monoterpene-emitting species is limited (e.g. Carriero et al., 2016; Mochizuchi et al., 2017). Hadacek et al. (2011) proposed that non-linear hormetic effects regulate the responses of stored secondary metabolites to abiotic factors, and that the reduction of ROS is a key step of the hormetic effects caused by these compounds. ROS are known to be stimulated by O<sub>3</sub> exposure (Pellegrini et al., 2019; Podda et al., 2019) as also shown in our date palms (data not shown). Overall, our results warrant more research on the redox chemistry of terpenoids under O<sub>3</sub> stress.

## Conclusions

This is the first experiment on date palm responses to chronic, realistic O<sub>3</sub> exposure. Significant declines of several gas exchange parameters and root biomass occurred only at the highest 2 x AA O<sub>3</sub> level. Some variables that are usually known as early responses to O<sub>3</sub> stress, responded already at 1.5 x AA. Isoprene emission did not appear to contribute to date palm O<sub>3</sub> tolerance as it declined at both elevated O<sub>3</sub> levels. In contrast, monoterpene emission was stimulated at 2 x AA and its O<sub>3</sub> responses should be further evaluated.

517 The major defense mechanisms that emerged from this study were avoidance of O<sub>3</sub> stress (i.e. exclusion of  
1  
518 O<sub>3</sub> entry by low maximum stomatal conductance to O<sub>3</sub> [73 mmol O<sub>3</sub> m<sup>-2</sup> s<sup>-1</sup>] and O<sub>3</sub>-induced stomatal  
3  
519 stomatal closure) and high capacity of catabolizing metabolites for detoxification and repair as indicated by  
4  
520 increased dark respiration. We thus conclude that this date palm cultivar was intermediately susceptible to  
6  
521 O<sub>3</sub>, but further studies with different cultivars are recommended as date palm cultivars may significantly  
10  
522 differ in their physiological traits such as stomatal conductance. These results are needed for a proper O<sub>3</sub>  
11  
12  
13  
523 risk assessment in the areas where *P. dactylifera* grows.  
15

524  
16  
17  
18  
525  
19

## 526 **Acknowledgments**

22  
23  
527  
24

528 We acknowledge: MITIMPACT project (INTERREG V A – Italy – France ALCOTRA); Fondazione Cassa di  
27  
529 Risparmio di Firenze for supporting the ozone FACE development; Barbara Mariotti for help during field  
29  
530 measurements; Cesare Garosi and Alessandra Marchica for biomass assessment; Moreno Lazzara for plant  
31  
531 cultivation; Alessandro Materassi, Francesco Sabatini and Gianni Fasano for ozone FACE maintenance. The  
34  
532 authors extend their appreciation to the Deanship of Scientific Research at King Saud University, Saudi  
35  
36  
533 Arabia, for partially funding this work through research group RG-1435-018. Financial support of L.A. by a  
37  
38  
534 short-term travelling grant of the Federation of European Societies of Plant Biology (FESPB) is gratefully  
41  
42  
535 acknowledged.  
43

44  
536  
46

## 537 **Conflict of interest**

48  
49  
538  
50

539 The authors declare that they have no conflicts of interest.  
53

540  
55

## 541 **Author contribution**

58  
542  
60

61  
62  
63  
64  
65

543 E. Paoletti, Y. Hoshika, L. Arab, and H. Rennenberg conceived the study and methodology, and Y. Hoshika, L.  
1  
544 Arab, S. Martini, L. Cotrozzi, D. Weber and P. Ache acquired data from the ozone FACE experiment; Y.  
3  
545 Hoshika and S. Martini contributed to the analysis of leaf gas exchange and biomass data; L. Neri and R.  
5  
546 Baraldi contributed to the analysis of BVOC emission; L. Cotrozzi and E. Pellegrini contributed to the  
8  
547 analysis of leaf pigments; D. Weber contributed to the analysis of chlorophyll fluorescence data; P. Ache, L.  
10  
548 Arab, H.M. Müller and R. Hedrich contributed to the analysis of RNA data; E. Paoletti, R. Hedrich, S. Alfarraj  
12  
549 and H. Rennenberg contributed to the interpretation of data to understand the date palm defense  
15  
550 mechanisms to ozone stress. E. Paoletti prepared the draft of the manuscript and all authors were involved  
17  
551 in writing the paper.  
20

21  
22  
23  
24  
25  
26  
27

## 28 **References**

29  
30  
31  
32

33 Agathokleous, E., Kitao, M. & Calabrese, E.J. (2018). Emission of volatile organic compounds from plants  
34 shows a biphasic pattern within an hormetic context. *Environmental Pollution* 239 ,318-321.  
35

36 Agathokleous, E., Saitanis, C. J., Wang, X., Watanabe, M., & Koike, T. (2016). A review study on past 40  
37 years of research on effects of tropospheric O<sub>3</sub> on belowground structure, functioning, and processes of  
38 trees: a linkage with potential ecological implications. *Water, Air, & Soil Pollution*, 227(1), 33.  
39

40 Aleid, S. M., Al-Khayri, J. M., & Al-Bahrany, A. M. (2015). Date palm status and perspective in Saudi Arabia.  
41 In Jain, S. M., & Johnson, D. V. (Eds.), *Date palm genetic resources and utilization* (pp. 49-95).  
42 Springer, Dordrecht.  
43

44 Arab, L., Cotrozzi, L., Lorenzini, G., Nali, C., Pellegrini, E., Hoshika, Y., Paoletti, E. & Rennenberg, H.  
45 Chronic ozone exposure modulates the foliar and root metabolome of date palm (*Phoenix dactylifera*)  
46 saplings. (in prep)  
47

48 Al-Jabr, A. M., Al-Khateeb, A. A., Al-Khateeb, S. A., & Al-Ayied, H. Y. (2007). Effects of Red Palm Weevil  
49 *Rynchophorus ferrugineus* (Olivier) infestation on gas exchange capacity of two date palm *Phoenix*  
50 *dactylifera* L. cultivars. *Journal of Biological Sciences*, 7, 1270-1273  
51

52  
53  
54  
55  
56  
57  
58  
59  
60  
61  
62  
63  
64  
65



- 571 Arab, L., Kreuzwieser, J., Kruse, J., Zimmer, I., Ache, P., Alfarraj, S., Al-Rasheid, K. A., Schnitzler, J.-P.,  
1  
572 Hedrich, R., & Rennenberg, H. (2016). Acclimation to heat and drought—Lessons to learn from the date  
3  
573 palm (*Phoenix dactylifera*). *Environmental and Experimental Botany*, 125, 20–30.  
5  
574 <https://doi.org/10.1016/j.envexpbot.2016.01.003>  
7  
575 Baraldi, R., Przybysz, A., Facini, O., Pierdonà, L., Carriero, G., Bertazza, G., & Neri, L. (2019). Impact of  
9  
576 drought and salinity on sweetgum tree (*Liquidambar styraciflua* L.): understanding tree ecophysiological  
11  
577 responses in the urban context. *Forests*, 10(11), 1032. <https://doi.org/10.3390/f10111032>  
13  
578 Böhm, J., Messerer, M., Müller, H. M., Scholz-Starke, J., Gradogna, A., Scherzer, S., ... & Ache, P. (2018).  
15  
579 Understanding the molecular basis of salt sequestration in epidermal bladder cells of *Chenopodium*  
17  
580 *quinoa*. *Current Biology*, 28(19), 3075–3085. <https://doi.org/10.1016/j.cub.2018.08.004>  
19  
581 Bussotti, F., Desotgiu, R., Cascio, C., Pollastrini, M., Gravano, E., Gerosa, G., Marzuoli, R., Nali, C.,  
21  
582 Lorenzini, G., Salvatori, E., Manes, F., Schaub, M., & Strasser, R. J. (2011). Ozone stress in woody  
23  
583 plants assessed with chlorophyll a fluorescence. A critical reassessment of existing data. *Environmental*  
25  
584 *and Experimental Botany*, 73(1), 19–30. <https://doi.org/10.1016/j.envexpbot.2010.10.022>  
27  
585 Butenhoff, C. L., Khalil, M. A. K., Porter, W. C., Al-Sahafi, M. S., Almazroui, M., & Al-Khalaf, A. (2015).  
29  
586 Evaluation of ozone, nitrogen dioxide, and carbon monoxide at nine sites in Saudi Arabia during 2007.  
31  
587 *Journal of the Air & Waste Management Association*, 65(7), 871–886.  
33  
588 <https://doi.org/10.1080/10962247.2015.1031921>  
35  
589 Carriero, G., Brunetti, C., Fares, S., Hayes, F., Hoshika, Y., Mills, G., ... & Paoletti, E. (2016). BVOC  
37  
590 responses to realistic nitrogen fertilization and ozone exposure in silver birch. *Environmental Pollution*,  
39  
591 213, 988–995. <https://doi.org/10.1016/j.envpol.2015.12.047>  
41  
592 Cascio, C., Schaub, M., Novak, K., Desotgiu, R., Bussotti, F., & Strasser, R. J. (2010). Foliar responses to  
43  
593 ozone of *Fagus sylvatica* L. seedlings grown in shaded and in full sunlight conditions. *Environmental*  
45  
594 *and Experimental Botany*, 68(2), 188–197. <https://doi.org/10.1016/j.envexpbot.2009.10.003>  
47  
595 Chen, S., Yang, J., Zhang, M., Strasser, R., & Qiang, S. (2016). Classification and characteristics of heat  
49  
596 tolerance in *Ageratina adenophora* populations using fast chlorophyll a fluorescence rise O-J-I-P.  
51  
597 *Environmental and Experimental Botany*, 122, 126–140.  
53  
598 <https://doi.org/10.1016/j.envexpbot.2015.09.011>  
55  
599 CLRTAP (2014). Mapping Critical Levels for Vegetation. In *Manual on methodologies and criteria for*  
57  
600 *modelling and mapping critical loads & levels and air pollution effects, risks and trends*. UNECE  
59  
601 Convention on Long-range Transboundary Air Pollution, ICP Modelling and Mapping.  
61  
62  
63  
64  
65

- 602 Close, D.C., Beadle, C.L. (2003) Alternate energy dissipation? Phenolic metabolites and the xanthophyll  
603 cycle. *Journal of Plant Physiology*, 160, 431-434.
- 604 Contran, N., Paoletti, E., Manning, W. J., & Tagliaferro, F. (2009). Ozone sensitivity and ethylenediurea  
605 protection in ash trees assessed by JIP chlorophyll a fluorescence transient analysis. *Photosynthetica*,  
606 47(1), 68–78. <https://doi.org/10.1007/s11099-009-0012-9>
- 607 Cotrozzi, L., Lorenzini, G., Nali, C., Pellegrini, E., Saponaro, V., Hoshika, Y., Arab, L., Rennenberg, H.,  
608 Paoletti, E. (2020). Hyperspectral reflectance of light-adapted leaves can predict both dark- and light-  
609 adapted Chl fluorescence parameters, and the effects of chronic ozone exposure on date palm  
610 (*Phoenix dactylifera*). *International Journal of Molecular Sciences* 21, 6441; doi:10.3390/ijms21176441
- 611 Cotrozzi, L., Campanella, A., Pellegrini, E., Lorenzini, G., Nali, C. & Paoletti, E. (2018a). Phenylpropanoids  
612 are key players in the antioxidant defense to ozone of European ash, *Fraxinus excelsior*. *Environmental*  
613 *Science and Pollution Research*, 25, 8137-8147. <https://doi.org/10.1007/s11356-016-8194-8>
- 614 Cotrozzi, L., Remorini, D., Pellegrini, E., Guidi, L., Nali, C., Lorenzini, G., ... & Landi, M. (2018b). Living in a  
615 Mediterranean city in 2050: broadleaf or evergreen 'citizens'?. *Environmental Science and Pollution*  
616 *Research*, 25(9), 8161-8173. <https://doi.org/10.1007/s11356-017-9316-7>
- 617 Desotgiu, R., Pollastrini, M., Cascio, C., Gerosa, G., Marzuoli, R., & Bussotti, F. (2013). Responses to ozone  
618 on Populus «Oxford» clone in an open top chamber experiment assessed before sunrise and in full  
619 sunlight. *Photosynthetica*, 51(2), 267–280. <https://doi.org/10.1007/s11099-012-0074-y>
- 620 Doaigey, A. R., Al-Wahaibi, M. H., Siddiqui, M. H., Al Sahli, A. A., & El-Zaidy, M. E. (2013). Effect of GA3 and  
621 2,4-D foliar application on the anatomy of date palm (*Phoenix dactylifera* L.) seedling leaf. *Saudi Journal*  
622 *of Biological Sciences*, 20(2), 141–147. <https://doi.org/10.1016/j.sjbs.2012.12.001>
- 623 Du, B., Kreuzwieser, J., Winkler, J. B., Ghirardo, A., Schnitzler, J.-P., Ache, P., Alfarraj, S., Hedrich, R.,  
624 White, P., & Rennenberg, H. (2018). Physiological responses of date palm (*Phoenix dactylifera*)  
625 seedlings to acute ozone exposure at high temperature. *Environmental Pollution*, 242, 905–913.  
626 <https://doi.org/10.1016/j.envpol.2018.07.059>
- 627 Esteban, R., Barrutia, O., Artetxe, U., Fernández-Marín, B., Hernández, A., & García-Plazaola, J. I. (2015).  
628 Internal and external factors affecting photosynthetic pigment composition in plants: a meta-analytical  
629 approach. *New Phytologist*, 206(1), 268-280. <https://doi.org/10.1111/nph.13186>
- 630 Fares, S., Loreto, F., Kleist, E. & Wildt, J. (2008). Stomatal uptake and stomatal deposition of ozone in  
631 isoprene and monoterpene emitting plants. *Plant Biology*, 10, 44-54. <https://doi.org/10.1055/s-2007-965257>

- 633 Feng, Z., Yuan, X., Fares, S., Loreto, F., Li, P., Hoshika, Y., & Paoletti, E. (2019). Isoprene is more affected  
1  
634 by climate drivers than monoterpenes: A meta-analytic review on plant isoprenoid emissions. *Plant, cell*  
3  
635 & *environment*, 42(6), 1939-1949. <https://doi.org/10.1111/pce.13535>  
5  
636 Fernandes, F. F., Esposito, M. P., da Silva Engela, M. R. G., Cardoso-Gustavson, P., Furlan, C. M., Hoshika,  
7  
637 Y., Carrari, E., Magni, G., Domingos, M., & Paoletti, E. (2019). The passion fruit liana (*Passiflora edulis*  
9  
638 Sims, Passifloraceae) is tolerant to ozone. *Science of The Total Environment*, 656, 1091–1101.  
11  
639 <https://doi.org/10.1016/j.scitotenv.2018.11.425>  
13  
640 Fry, M. M., Naik, V., West, J. J., Schwarzkopf, M. D., Fiore, A. M., Collins, W. J., Dentener, F. J., Shindell, D.  
15  
641 T., Atherton, C., Bergmann, D., Duncan, B. N., Hess, P., MacKenzie, I. A., Marmer, E., Schultz, M. G.,  
17  
642 Szopa, S., Wild, O., & Zeng, G. (2012). The influence of ozone precursor emissions from four world  
19  
643 regions on tropospheric composition and radiative climate forcing. *Journal of Geophysical Research:*  
21  
644 *Atmospheres*, 117(D7). <https://doi.org/10.1029/2011JD017134>  
23  
645 Gao, F., Catalayud, V., Paoletti, E., Hoshika, Y., & Feng, Z. (2017). Water stress mitigates the negative  
25  
646 effects of ozone on photosynthesis and biomass in poplar plants. *Environmental Pollution*, 230, 268-  
27  
647 279. <https://doi.org/10.1016/j.envpol.2017.06.044>Geron, C., Harley, P. & Guenther, A. (2001). Isoprene  
29  
648 emission capacity for US tree species. *Atmospheric Environment* 35, 3341-3352  
31  
649 [https://doi.org/10.1016/S1352-2310\(00\)00407-6](https://doi.org/10.1016/S1352-2310(00)00407-6)  
33  
650 Grulke, N. E., & Heath, R. L. (2020). Ozone effects on plants in natural ecosystems. *Plant Biology*, 22, 12-  
35  
651 37. <https://doi.org/10.1111/plb.12971>  
37  
652 Guenther, A. B., Jiang, X., Heald, C. L., Sakulyanontvittaya, T., Duhl, T., Emmons, L. K., & Wang, X. (2012).  
39  
653 The Model of Emissions of Gases and Aerosols from Nature version 2.1 (MEGAN2. 1): an extended  
41  
654 and updated framework for modeling biogenic emissions. *Geoscientific Model Development* 5(6): 1471–  
43  
655 1492.  
45  
656 Guéra, A., Calatayud, A., Sabater, B., & Barreno, E. (2005). Involvement of the thylakoidal NADH-  
47  
657 plastoquinone-oxidoreductase complex in the early responses to ozone exposure of barley (*Hordeum*  
49  
658 *vulgare* L.) seedlings. *Journal of Experimental Botany*, 56(409), 205–218.  
51  
659 <https://doi.org/10.1093/jxb/eri024>  
53  
660 Guidi, L., Lo Piccolo, E. & Landi, M. (2019) Chlorophyll fluorescence, photoinhibition and abiotic stress: Does  
55  
661 it make any difference the fact to be a C3 or C4 species? *Frontiers in Plant Science*, 10, 174.  
57  
662 <https://doi.org/10.3389/fpls.2019.00174>  
59  
60  
61  
62  
63  
64  
65

- 663 Hadacek, F., Bachmann, G., Engelmeier, D., & Chobot, V. (2011). Hormesis and a chemical raison d'être for  
664 secondary plant metabolites. *Dose-response*, 9(1), dose-response. [https://doi.org/10.2203/dose-  
666 response.09-028.Hadacek](https://doi.org/10.2203/dose-<br/>665 response.09-028.Hadacek)
- 666 Harvey, C.M. & Sharkey, T.D. (2016). Exogenous isoprene modulates gene expression in unstressed  
667 *Arabidopsis thaliana* plants. *Plant, Cell and Environment*, 39, 1251–1263.  
668 <https://doi.org/10.1111/pce.12660>
- 669 Harvey, C. M., Li, Z., Tjellström, H., Blanchard, G. J., & Sharkey, T. D. (2015). Concentration of isoprene in  
670 artificial and thylakoid membranes. *Journal of Bioenergetics and Biomembranes*, 47(5), 419-429.  
671 <https://doi.org/10.1007/s10863-015-9625-9>
- 672 Heckathorn, S. A., Coleman, J. S., & Hallberg, R. L. (1998). Recovery of net CO<sub>2</sub> assimilation after heat  
673 stress is correlated with recovery of oxygen-evolving-complex proteins in *Zea mays* L. In  
674 *Photosynthetica*. 34, 13–20. <https://doi.org/10.1023/A:1006899314677>
- 675 Hewitt, C. N., MacKenzie, A. R., Carlo, P. D., Marco, C. F. D., Dorsey, J. R., Evans, M., Fowler, D.,  
676 Gallagher, M. W., Hopkins, J. R., Jones, C. E., Langford, B., Lee, J. D., Lewis, A. C., Lim, S. F.,  
677 McQuaid, J., Misztal, P., Moller, S. J., Monks, P. S., Nemitz, E., ... Stewart, D. J. (2009). Nitrogen  
678 management is essential to prevent tropical oil palm plantations from causing ground-level ozone  
679 pollution. *Proceedings of the National Academy of Sciences*, 106(44), 18447–18451.  
680 <https://doi.org/10.1073/pnas.0907541106>
- 681 Hoshika, Y., De Carlo, A., Baraldi, R., Neri, L., Carrari, E., Agathokleous, E., Zhang, L., Fares, S. & Paoletti,  
682 E. (2019) Ozone-induced impairment of night-time stomatal closure in O<sub>3</sub>-sensitive poplar clone is  
683 affected by nitrogen but not by phosphorus enrichment. *Science of the Total Environment*, 692, 713-  
684 722. <https://doi.org/10.1016/j.scitotenv.2019.07.288>
- 685 Hoshika, Y., Fares, S., Pellegrini, E., Conte, A., & Paoletti, E. (2020a). Water use strategy affects avoidance  
686 of ozone stress by stomatal closure in Mediterranean trees—A modelling analysis. *Plant, Cell &  
687 Environment*, 43(3), 611–623. <https://doi.org/10.1111/pce.13700>
- 688 Hoshika, Y., Haworth, M., Watanabe, M. & Koike, T. (2020b). Interactive effect of leaf age and ozone on  
689 mesophyll conductance in Siebold's beech. *Physiologia Plantarum*, 170(2), 172–186.  
690 <https://doi.org/10.1111/ppl.13121>
- 691 Hoshika, Y., Osada, Y., De Marco, A., Penuelas, J., & Paoletti, E. (2018). Global diurnal and nocturnal  
692 parameters of stomatal conductance in woody plants and major crops. *Global ecology and  
693 biogeography*, 27(2), 257-275. <https://doi.org/10.1111/geb.12681>

- 694 Hu, S., Ding, Y., & Zhu, C. (2020). Sensitivity and responses of chloroplasts to heat stress in plants.  
695 *Frontiers in Plant Science*, 11(April), 1–11. <https://doi.org/10.3389/fpls.2020.00375>
- 696 Kalaji, H. M., Schansker, G., Brestic, M., Bussotti, F., Calatayud, A., Ferroni, L., ... & Losciale, P. (2017).  
697 Frequently asked questions about chlorophyll fluorescence, the sequel. *Photosynthesis Research*,  
698 132(1), 13-66. <https://doi.org/10.1007/s11120-016-0318-y>
- 699 Kesselmeier, J., & Staudt, M. (1999). Biogenic volatile organic compounds (VOC): an overview on emission,  
700 physiology and ecology. *Journal of atmospheric chemistry*, 33(1), 23-88.
- 701 Kitao, M., Löw, M., Heerdt, C., Grams, T.E.E., Häberle, K.-H. & Matyssek, R. (2009). Effects of chronic  
702 elevated ozone exposure on gas exchange responses of adult beech trees (*Fagus sylvatica*) as related  
703 to the within-canopy light gradient. *Environmental Pollution*, 157, 537-544.  
704 <https://doi.org/10.1016/j.envpol.2008.09.016>
- 705 Kruse, J., Adams, M. A., Kadinov, G., Arab, L., Kreuzwieser, J., Alfarraj, S., ... & Rennenberg, H. (2017).  
706 Characterization of photosynthetic acclimation in *Phoenix dactylifera* by a modified Arrhenius equation  
707 originally developed for leaf respiration. *Trees*, 31(2), 623-644. <https://doi.org/10.1111/nph.15923>
- 708 Kruse, J., Adams, M., Winkler, B., Ghirardo, A., Alfarraj, S., Kreuzwieser, J., ... & Rennenberg, H. (2019).  
709 Optimization of photosynthesis and stomatal conductance in the date palm *Phoenix dactylifera* during  
710 acclimation to heat and drought. *New Phytologist*, 223(4), 1973-1988.
- 711 Kulshrestha, U., & Kumar, B. (2014). Airmass Trajectories and Long Range Transport of Pollutants: Review  
712 of Wet Deposition Scenario in South Asia. *Advances in Meteorology*; Hindawi.  
713 <https://doi.org/10.1155/2014/596041>
- 714 Lantz, A. T., Allman, J., Weraduwege, S. M., & Sharkey, T. D. (2019). Isoprene: New insights into the control  
715 of emission and mediation of stress tolerance by gene expression. *Plant, Cell & Environment*, 42(10),  
716 2808-2826. <https://doi.org/10.1111/pce.13629>
- 717 Lelieveld, J., Hoor, P., Jockel, P., Pozzer, A., & Hadjinicolaou, P. (2009). Severe ozone air pollution in the  
718 Persian Gulf region. *Atmos. Chem. Phys.*, 14.
- 719 Li, P., Feng, Z., Catalayud, V., Yuan, X., Xu, Y., & Paoletti, E. (2017). A meta-analysis on growth,  
720 physiological, and biochemical responses of woody species to ground-level ozone highlights the role of  
721 plant functional types. *Plant, Cell & Environment*, 40(10), 2369–2380. <https://doi.org/10.1111/pce.13043>

- 722 Loreto, F., & Velikova, V. (2001). Isoprene produced by leaves protects the photosynthetic apparatus against  
1  
723 ozone damage, quenches ozone products, and reduces lipid peroxidation of cellular membranes. *Plant*  
2  
724 *Physiology*, 127(4), 1781–1787. <https://doi.org/10.1104/pp.010497>  
3  
4  
5  
725 Matsubara, S., & Chow, W. S. (2004). Populations of photoinactivated photosystem II reaction centers  
6  
726 characterized by chlorophyll a fluorescence lifetime in vivo. *Proceedings of the National Academy of*  
7  
827 *Sciences of the United States of America*, 101(52), 18234–18239.  
9  
1028 <https://doi.org/10.1073/pnas.0403857102>  
11  
12  
13  
1429 Mereu, S., Gerosa, G., Marzuoli, R., Fusaro, L., Salvatori, E., Finco, A., Spano, D., & Manes, F. (2011). Gas  
15  
1630 exchange and JIP-test parameters of two Mediterranean maquis species are affected by sea spray and  
17  
1831 ozone interaction. *Environmental and Experimental Botany*, 73, 80–88.  
19  
2032 <https://doi.org/10.1016/j.envexpbot.2011.02.004>  
21  
22  
2333 Mills, G., Pleijel, H., Malley, C. S., Sinha, B., Cooper, O. R., Schultz, M. G., ... & Gerosa, G. (2018).  
23  
2434 Tropospheric Ozone Assessment Report: Present-day tropospheric ozone distribution and trends  
25  
2635 relevant to vegetation. *Elem Sci Anth*, 6(1)  
27  
2836 Mochizuki, T., Watanabe, M., Koike, T., Tani, A. (2017). Monoterpene emissions from needles of hybrid larch  
29  
3037 F<sub>1</sub> (*Larix gmelinii* var. *japonica* × *Larix kaempferi*) grown under elevated carbon dioxide and ozone.  
31  
3238 *Atmospheric Environment* 148, 197-202  
33  
3439 Moldau, H. (1998). Hierarchy of ozone scavenging reactions in the plant cell wall. *Physiologia Plantarum*,  
35  
3640 104(4), 617-622. <https://doi.org/10.1034/j.1399-3054.1998.1040414.x>  
37  
38  
3941 Moura, B. B., Hoshika, Y., Silveira, N. M., Marcos, F. C. C., Machado, E. C., Paoletti, E., & Ribeiro, R. V.  
40  
4142 (2018). Physiological and biochemical responses of two sugarcane genotypes growing under free-air  
42  
4343 ozone exposure. *Environmental and Experimental Botany*, 153, 72–79.  
44  
4544 <https://doi.org/10.1016/j.envexpbot.2018.05.004>  
46  
4745 Mrak, T., Štraus, I., Grebenc, T., Gričar, J., Hoshika, Y., Carriero, G., ... & Kraigher, H. (2019). Different  
48  
4946 belowground responses to elevated ozone and soil water deficit in three European oak species  
50  
5147 (*Quercus ilex*, *Q. pubescens* and *Q. robur*). *Science of the total environment*, 651, 1310-1320.  
52  
5348 <https://doi.org/10.1016/j.scitotenv.2018.09.246>  
54  
5549 Niinemets, Ü., Kollist, H., García-Plazaola, J.I., Hernández, A., Becerril, J.M. (2003). Do the capacity and  
56  
5750 kinetics for modification of xanthophyll cycle pool size depend on growth irradiance in temperature  
58  
5951 trees? *Plant, Cell & Environment*, 26, 1787-1802.  
60  
61  
62  
63  
64  
65

- 752 Ohara, T., Akimoto, H., Kurokawa, J., Horii, N., Yamaji, K., Yan, X., & Hayasaka, T. (2007). An Asian  
1  
753 emission inventory of anthropogenic emission sources for the period 1980-2020. *Atmospheric*  
2  
754 *Chemistry and Physics Discussions*, 7(3), 6843–6902.
- 5  
755 Oukarroum, A., El Madidi, S., Schansker, G., & Strasser, R. J. (2007). Probing the responses of barley  
7  
756 cultivars (*Hordeum vulgare* L.) by chlorophyll a fluorescence OLKJIP under drought stress and re-  
8  
9  
1077 watering. *Environmental and Experimental Botany*, 60(3), 438-446.  
11  
1758 <https://doi.org/10.1016/j.envexpbot.2007.01.002>
- 13  
1759 Oukarroum, A., Schansker, G., & Strasser, R. J. (2009). Drought stress effects on photosystem I content and  
15  
1760 photosystem II thermotolerance analyzed using Chl a fluorescence kinetics in barley varieties differing  
17  
1761 in their drought tolerance. *Physiologia Plantarum*, 137(2), 188–199. [https://doi.org/10.1111/j.1399-  
19  
2762 3054.2009.01273.x](https://doi.org/10.1111/j.1399-3054.2009.01273.x)
- 21  
2763 Paoletti, E. (2005) Ozone slows stomatal response to light and leaf wounding in a Mediterranean evergreen  
23  
2764 broadleaf, *Arbutus unedo*. *Environmental Pollution*, 134, 439–445.  
25  
2765 <https://doi.org/10.1016/j.envpol.2004.09.011>
- 27  
28  
2766 Paoletti, E. (2006). Impact of ozone on Mediterranean forests: A review. *Environmental Pollution*, 144(2),  
30  
3767 463–474. <https://doi.org/10.1016/j.envpol.2005.12.051>
- 32  
3768 Paoletti, E. (2007). Ozone impacts on forests. *CAB Reviews: Perspectives in Agriculture, Veterinary Science,*  
34  
3769 *Nutrition and Natural Resources*, 2(068). <https://www.cabdirect.org/cabdirect/abstract/20083055513>
- 36  
3770 Paoletti, E., Materassi, A., Fasano, G., Hoshika, Y., Carriero, G., Silaghi, D., & Badea, O. (2017). A new-  
38  
3771 generation 3D ozone FACE (Free Air Controlled Exposure). *Science of The Total Environment*, 575,  
40  
4772 1407–1414. <https://doi.org/10.1016/j.scitotenv.2016.09.217>
- 42  
4773 Papageorgiou, G. C., & Govindjee, G. C. (2004). Chlorophyll a fluorescence: a signature of photosynthesis  
44  
4774 (advances in photosynthesis and respiration). In *Adv Photosynth Respir* (Vol. 19, p. 818). Springer  
46  
4775 Dordrecht, The Netherlands.
- 48  
4776 Parra, R. (2008). Contribution of oil palm isoprene emissions to tropospheric ozone levels in the Distrito  
50  
5777 Metropolitano de Quito (Ecuador). In *Air Pollution. Sixteen International Conference on Modeling,*  
52  
5778 *Monitoring and Management of Air Pollution* (pp. 95-104).
- 54  
5779 Patankar, H., M. Assaha, D. V., Al-Yahyai, R., Sunkar, R., & Yaish, M. W. (2016). Identification of reference  
56  
5780 genes for quantitative real-time PCR in date palm (*Phoenix dactylifera* L.) subjected to drought and  
58  
5781 salinity. *PloS one*, 11(11), e0166216. <https://doi.org/10.1371/journal.pone.0166216>
- 60  
61  
62  
63  
64  
65

- 782 Pellegrini, E., Francini, A., Lorenzini, G. & Nali, C. (2011). PSII photochemistry and carboxylation efficiency  
1  
783 in *Liriodendron tulipifera* under ozone exposure. *Environmental and Experimental Botany*, 70, 217-226.  
2  
784 <https://doi.org/10.1016/j.envexpbot.2010.09.012>  
3
- 785 Pellegrini, E., Hoshika, Y., Dusart, N., Cotrozzi, L., Gérard, J., Nali, C., ... & Paoletti, E. (2019). Antioxidative  
7 responses of three oak species under ozone and water stress conditions. *Science of the total*  
786 *environment*, 647, 390-399. <https://doi.org/10.1016/j.scitotenv.2018.07.413>  
9  
1077
- 11  
1788 Podda, A., Pisuttu, C., Hoshika, Y., Pellegrini, E., Carrari, E., Lorenzini, G., ... & Neri, L. (2019). Can nutrient  
12  
1789 fertilization mitigate the effects of ozone exposure on an ozone-sensitive poplar clone?. *Science of the*  
13  
1790 *Total Environment*, 657, 340-350. <https://doi.org/10.1016/j.scitotenv.2018.11.459>  
15  
1791
- 1791 Pollastri, S., Jorba, I., Hawkins, T.J., Llusiá, J., Michelozzi, M., Navajas, D., Peñuelas, J., Hussey, P.J.,  
19  
2792 Knight, M.R. & Loreto, F. (2019). Leaves of isoprene-emitting tobacco plants maintain PSII stability at  
21  
2793 high temperatures. *New Phytologist*, 223, 1307–1318. <https://doi.org/10.1111/nph.15847>  
23  
24
- 2794 R Core Team (2018) R: A language and environment for statistical computing. Vienna, Austria: R Foundation  
26  
2795 for Statistical Computing. Retrieved from <https://www.R-project.org/>  
28
- 2796 Radaideh, J. A. (2016). Industrial air pollution in Saudi Arabia and the influence of meteorological variables.  
30  
3797 *Environmental Science and Technology*, 1, 334.  
32
- 3798 Rapparini, F., Baraldi, R., Miglietta, F., & Loreto, F. (2004). Isoprenoid emission in trees of *Quercus*  
34  
3799 *pubescens* and *Quercus ilex* with lifetime exposure to naturally high CO<sub>2</sub> environment. *Plant, Cell &*  
36  
3800 *Environment*, 27(4), 381-391. <https://doi.org/10.1111/j.1365-3040.2003.01151.x>  
38
- 3801 Reich, P. B. (1987). Quantifying plant response to ozone: a unifying theory. *Tree physiology*, 3(1), 63-91.  
40
- 4802 Salvatori, E., Fusaro, L., Mereu, S., Bernardini, A., Puppi, G., & Manes, F. (2013). Different O<sub>3</sub> response of  
42  
4803 sensitive and resistant snap bean genotypes (*Phaseolus vulgaris* L.): The key role of growth stage,  
44  
4804 stomatal conductance, and PSI activity. *Environmental and Experimental Botany*, 87, 79–91.  
46  
4805 <https://doi.org/10.1016/j.envexpbot.2012.09.008>  
48
- 4806 Schansker, G., Tóth, S. Z., & Strasser, R. J. (2005). Methylviologen and dibromothymoquinone treatments of  
50  
51  
507 pea leaves reveal the role of photosystem I in the Chl a fluorescence rise OJIP. *Biochimica et*  
52  
53  
508 *Biophysica Acta - Bioenergetics*, 1706(3), 250–261. <https://doi.org/10.1016/j.bbabi.2004.11.006>  
54
- 55  
509 Schansker, G., Tóth, S. Z., & Strasser, R. J. (2006). Dark recovery of the Chl a fluorescence transient (OJIP)  
56  
57  
810 after light adaptation: The qT-component of non-photochemical quenching is related to an activated  
58  
59  
60  
61  
62  
63  
64  
65



811 photosystem I acceptor side. *Biochimica et Biophysica Acta - Bioenergetics*, 1757(7), 787–797.  
812 <https://doi.org/10.1016/j.bbabi.2006.04.019>

813 Smoydzin, L., Fnais, M., & Lelieveld, J. (2012). Ozone pollution over the Arabian Gulf—Role of  
814 meteorological conditions. *Atmospheric Chemistry & Physics Discussions*, 12, 6331–6361.  
815 <https://doi.org/10.5194/acpd-12-6331-2012>

816 Sperling, O., Shapira, O., Tripler, E., Schwartz, A., & Lazarovitch, N. (2014). A model for computing date  
817 palm water requirements as affected by salinity. *Irrigation science*, 32(5), 341–350.

818 Strasser, R. J., Tsimilli-Michael, M., Qiang, S., & Goltsev, V. (2010). Simultaneous in vivo recording of  
819 prompt and delayed fluorescence and 820-nm reflection changes during drying and after rehydration of  
820 the resurrection plant *Haberlea rhodopensis*. *Biochimica et Biophysica Acta*, 1797(6–7), 1313–1326.  
821 <https://doi.org/10.1016/j.bbabi.2010.03.008>

822 Takagi, D., Ishizaki, K., Hanawa, H., Mabuchi, T., Shimakawa, G., Yamamoto, H. & Miyake, C. (2017).  
823 Diversity of strategies for escaping reactive oxygen species production within photosystem I among land  
824 plants: P700 oxidation system is prerequisite for alleviating photoinhibition in photosystem I. *Physiologia*  
825 *Plantarum*, 161, 56–74. <https://doi.org/10.1111/ppl.12562>

826 Tóth, S. Z., Schansker, G., & Strasser, R. J. (2007). A non-invasive assay of the plastoquinone pool redox  
827 state based on the OJIP-transient. *Photosynthesis Research*, 93(1–3), 193–203.  
828 <https://doi.org/10.1007/s11120-007-9179-8>

829 Tsimilli-Michael, M., & Strasser, R. (2008). In vivo Assessment of Stress Impact on Plant's Vitality:  
830 Applications in Detecting and Evaluating the Beneficial Role of Mycorrhization on Host Plants. In Varma  
831 A. (Eds.), *Mycorrhiza* (pp. 679–703). Springer, Berlin, Heidelberg. [https://doi.org/10.1007/978-3-540-](https://doi.org/10.1007/978-3-540-78826-3_32)  
832 [78826-3\\_32](https://doi.org/10.1007/978-3-540-78826-3_32)

833 Van Heerden, P. D. R., Strasser, R. J., & Krüger, G. H. J. (2004). Reduction of dark chilling stress in N<sub>2</sub>-  
834 fixing soybean by nitrate as indicated by chlorophyll a fluorescence kinetics. *Physiologia Plantarum*,  
835 121(2), 239–249. <https://doi.org/10.1111/j.0031-9317.2004.0312.x>

836 Velikova, V., Tsonev, T., Pinelli, P., Alessio, G. A., & Loreto, F. (2005). Localized ozone fumigation system  
837 for studying ozone effects on photosynthesis, respiration, electron transport rate and isoprene emission  
838 in field-grown Mediterranean oak species. *Tree Physiology*, 25(12), 1523–1532.  
839 <https://doi.org/10.1093/treephys/25.12.1523>

- 840 Vickers, C.E., Possell, M., Velkova, V.B., Laothawornkitkul, J., Ryan, A., Mullineaux, P.M. & Hewitt, C.N.  
841 (2009). Isoprene synthesis protects transgenic tobacco plants from oxidative stress. *Plant, Cell and*  
842 *Environment*, 32, 520–531. <https://doi.org/10.1111/j.1365-3040.2009.01946.x>
- 843 Watanabe, M., Hoshika, Y., Inada, N., Wang, X., Mao, Q. & Koike, T. (2013). Photosynthetic traits of  
844 Siebold's beech and oak saplings grown under free air ozone exposure. *Environmental Pollution*, 174,  
845 50-56. <https://doi.org/10.1016/j.envpol.2012.11.006>
- 846 Weraduwege, S. M., Micallef, B. J., Grodzinski, B., Taylor, D. C., & Marillia, E. F. (2011). Roles of dark  
847 respiration in plant growth and productivity. In Moo-Young M. (Eds.), *Comprehensive biotechnology 2<sup>nd</sup>*  
848 *Ed.*, pp. 191-207. Elsevier
- 849 Yuan, X., Calatayud, V., Gao, F., Fares, S., Paoletti, E., Tian, Y., & Feng, Z. (2016). Interaction of drought  
850 and ozone exposure on isoprene emission from extensively cultivated poplar. *Plant, Cell &*  
851 *Environment*, 39(10), 2276-2287. <https://doi.org/10.1111/pce.12798>
- 852 Zhang, L., Hoshika, Y., Carrari, E., Cotrozzi, L., Pellegrini, E. & Paoletti, E. (2018a). Effects of nitrogen and  
853 phosphorus imbalance on photosynthetic traits of poplar Oxford clone under ozone pollution. *Journal of*  
854 *Plant Research*, 131, 915-924. <https://doi.org/10.1007/s10265-018-1071-4>
- 855 Zhang, L., Hoshika, Y., Carrari, E., Burkey, K. O., & Paoletti, E. (2018b). Protecting the photosynthetic  
856 performance of snap bean under free air ozone exposure. *Journal of Environmental Sciences*, 66, 31-  
857 40. <https://doi.org/10.1016/j.jes.2017.05.009>
- 858 Živčák, M., Olšovská, K., Slamka, P., Galambošová, J., Rataj, V., Shao, H. B., & Brestič, M. (2014).  
859 Application of chlorophyll fluorescence performance indices to assess the wheat photosynthetic  
860 functions influenced by nitrogen deficiency. *Plant, Soil and Environment*, 60(5), 210–215.  
861 <https://doi.org/10.17221/73/2014-pse>
- 862 Zuo, Z., Weraduwege, S.M., Lantz, A.T., Sanchez, L.M., Weise, S.E., Wang, J., Childs, K.L. & Sharkey, T.D.  
863 (2019). Isoprene acts as a signaling molecule in gene networks important for stress responses and  
864 plant growth. *Plant Physiology*, 180, 124–152. <https://doi.org/10.1104/pp.18.01391>

866 **Figure and table legends**

1  
867 **Fig. 1.** Environmental conditions over the experimental period (from May 20<sup>th</sup> to August 20<sup>th</sup>, 2019 = 92  
3  
868 days of exposure). a) Daily averages of temperature (Temp), vapor pressure deficit (VPD), photosynthetic  
4  
5  
6  
869 active solar radiation (PAR), and precipitation. b) Daily ozone averages and AOT40 and POD1 values in the  
8  
870 three ozone treatments, i.e. ambient air (AA), 1.5 x AA and 2 x AA.

10  
11  
871 **Fig. 2.** Relationship between stomatal conductance ( $g_s$ ) and leaf-to-air vapor pressure deficit (VPD) in date  
12  
13  
872 palm leaves grown under different O<sub>3</sub> concentrations (AA, ambient, 1.5 x AA, 2 x AA). Data were obtained  
15  
16  
873 under a PPFD > 1000  $\mu\text{mol m}^{-2} \text{s}^{-1}$ . Simple linear regression analyses were applied: \*\*\*  $p < 0.001$ , \*\*  $p <$   
17  
18  
874 0.01, ns denotes not significant. Since the regressions were statistically significant for AA and 1.5 x AA, we  
20  
21  
875 applied the ANCOVA; \*  $p < 0.05$ , ns denotes not significant.

22  
23  
876 **Fig. 3.** Average ( $\pm$  standard error) of dark respiration rate ( $R_n$ ) on July 30<sup>th</sup>. Different letters show significant  
24  
25  
877 effects of the ozone treatments (AA, ambient, 1.5 x AA, 2 x AA) (Tukey test,  $p < 0.05$ , N = 3 plots).

27  
28  
878 **Fig. 4.** Effect of different ozone levels on date palms, assessed with Chlorophyll-a fluorescence  
29  
30  
879 measurements *in vivo*. Boxplots show differences between elevated ozone levels compared to ambient  
31  
32  
880 ozone level (AA). Orange boxes, 1.5 x AA; red boxes, 2 x AA. Whiskers: 1,5 x IQR, dots: outliers, cross:  
34  
35  
881 average, line: median; green dotted line at  $y = 0$ : reference value at ambient ozone level; n = 3 plots. (a)  
36  
37  
882  $\Delta W_L$  difference of variable fluorescence  $\Delta W_{OK}$ , at the L-Step at  $t = 150 \mu\text{s}$ . (b) difference of variable  
38  
39  
883 fluorescence  $\Delta W_{O_1}$ , at the K-Step  $t = 300-600 \mu\text{s}$ . (c) difference of variable fluorescence  $\Delta V$ , at the J-Step  $t =$   
41  
42  
884 2 ms. (d) difference of variable fluorescence  $\Delta V$ , at the I-Step  $t = 30 \text{ ms}$ .

44  
45  
885 **Fig. 5.** Effect of different ozone levels on date palms on (a) maximum quantum yield for primary  
46  
47  
886 photochemistry  $\phi_{P_0}$  (b) the performance index  $PI_{TOT}$ , (c) energy dissipation per active reaction centres  
48  
49  
887  $DI_0/RC$ , (d) reaction centres per absorption  $10RC/ABS$ . Boxplots show: Green boxes, ambient ozone level  
51  
52  
888 (AA); orange boxes, 1.5 x AA; red boxes, 2 x AA. Whiskers: 1,5 x IQR, dots: outliers, cross: average, line:  
53  
54  
889 median. Different letters show significant differences among treatments (Tukey test,  $p < 0.05$ , N = 3 plots).

55  
56  
890 **Fig. 6.** Average ( $\pm$  standard error) of isoprene emission (a), relative expression of isoprene synthase  
58  
59  
891 transcripts (b), monoterpene emission (c), relative expression of monoterpene synthases (d) and total  
60  
61  
62  
63  
64  
65

892 volatile organic compounds (VOC) emission (e) in date palm leaves on 1-2 August. Different letters show  
1  
893 significant effects of the ozone treatments (AA, ambient, 1.5 x AA, 2 x AA) (Tukey test,  $p < 0.05$ ,  $N = 3$  plots).  
3

894 **Fig. 7.** Relationships between BVOC emission and net photosynthesis (a, isoprene; c, monoterpene),  
4  
5  
6  
895 intercellular CO<sub>2</sub> concentration (b, isoprene; d, monoterpene) in date palm leaves grown under different O<sub>3</sub>  
8  
896 concentrations (AA, ambient, 1.5 x AA, 2 x AA). Simple linear regression analyses: \*\*  $p < 0.01$ , \*  $p < 0.05$ , ns  
10  
11  
897 denotes not significant.  
12

898 **Fig. 8** Above- (a) and below-ground (b) biomass of date palms on August 20<sup>th</sup>, i.e. at the end of 92 days of  
15  
16  
899 exposure to ambient ozone (AA), 1.5 x AA and 2 x AA. Different letters show significant differences among  
17  
18  
900 treatments (Tukey test,  $p < 0.05$ ,  $N = 3$  plots).  
19  
20

901  
22  
23  
902  
24  
25  
903 **Tab. 1.** Mass per area (LMA), water content (LWC), total chlorophyll content (Chl<sub>TOT</sub>), chlorophyll a/b ratio  
27  
904 (Chl a/b), total carotenoid content (Car<sub>TOT</sub>), β-carotene (β-car), lutein (Lut), xanthophyll cycle pigment  
29  
905 content (VAZ) and de-epoxidation state (DEPS) in the leaves of date palm plants grown under three levels  
31  
32  
906 of O<sub>3</sub> concentration (AA, ambient O<sub>3</sub> concentration, 1.5 × AA, 2 × AA). Each value is the mean ± standard  
34  
35  
907 error ( $N = 3$  plots). Asterisks show the significance of ANOVA: \*\*  $p < 0.01$ , \*  $p < 0.05$ , ns denotes not  
36  
37  
908 significant. Different letters show significant differences among treatments ( $p < 0.05$ , Tukey test).  
38  
39

40  
909 **Tab 2.** Average (± standard error) of the daily profiles of net photosynthesis (A) and stomatal conductance  
42  
43  
910 ( $g_s$ ) of date palm leaves on July 23<sup>rd</sup> and 30<sup>th</sup> 2019. Asterisks show the significance of two-way ANOVA: \*\*  $p$   
44  
45  
911 < 0.01; \*  $p < 0.05$ ; ns, not significant. Different capital letters show results of a one-way ANOVA with  
46  
47  
912 daytime as a factor, while different lower-case letters show results of a one-way ANOVA with O<sub>3</sub>  
49  
50  
913 treatments (AA, ambient, 1.5 x AA, 2 x AA) within each daytime as a factor (Tukey test,  $p < 0.05$ ,  $N = 3$  plots).  
51  
52

914

915

56

57

58

59

60

61

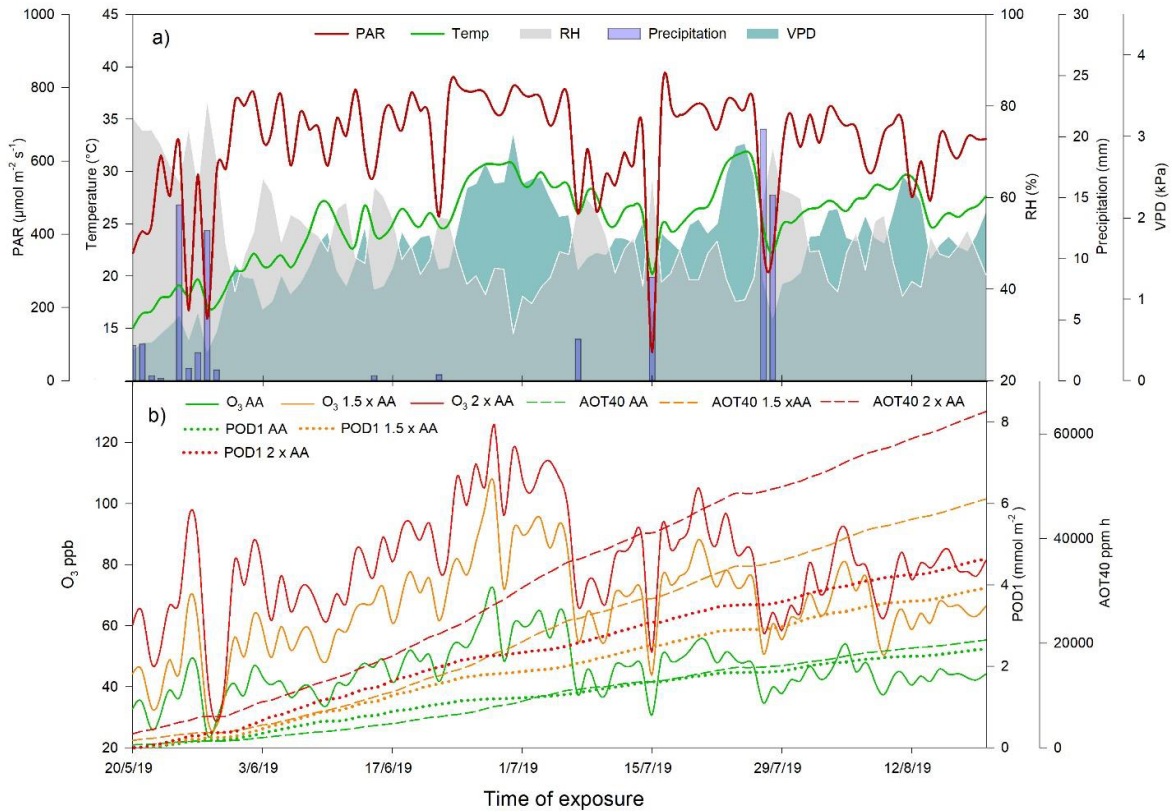
62

63

64

65

916 **Figures and Tables**



917  
 918 **Fig. 1** Environmental conditions over the experimental period (from May 20<sup>th</sup> to August 20<sup>th</sup>, 2019 = 92 days  
 919 of exposure). a) Daily averages of temperature (Temp), vapor pressure deficit (VPD), photosynthetic active  
 920 solar radiation (PAR), and precipitation. b) Daily ozone averages and AOT40 and POD1 values in the three  
 921 ozone treatments, i.e. ambient air (AA), 1.5 x AA and 2 x AA.

923

1  
2  
3  
4  
5  
6  
7  
8  
9  
10  
11  
12  
13  
14  
15  
16  
17  
18  
19  
20  
21  
22  
23  
24  
25  
26  
27  
28  
29  
30  
31  
32  
33  
34  
35  
36  
37  
38  
39  
40  
41  
42  
43  
44  
45  
46  
47  
48  
49  
50  
51  
52  
53  
54  
55  
56  
57  
58  
59  
60  
61  
62  
63  
64  
65

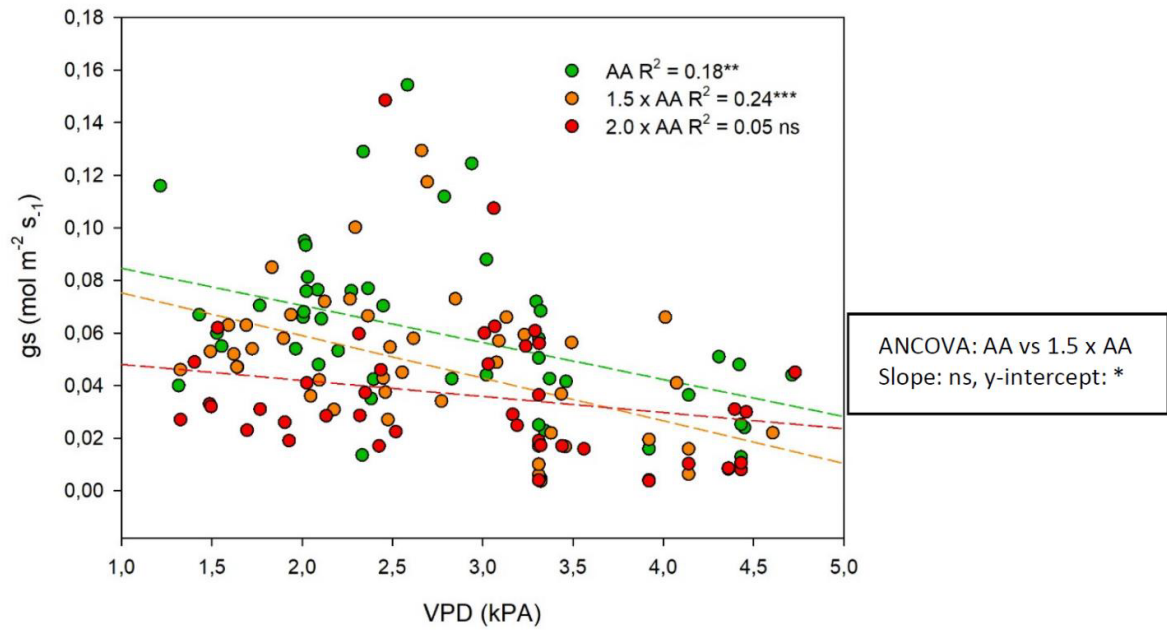


**Fig. 2.** Relationship between stomatal conductance ( $g_s$ ) and leaf-to-air vapor pressure deficit (VPD) in date palm leaves grown under different  $O_3$  concentrations (AA, ambient, 1.5 x AA, 2 x AA). Data were obtained under a PPFD > 1000  $\mu\text{mol m}^{-2} \text{s}^{-1}$ . Simple linear regression analyses were applied: \*\*\*  $p < 0.001$ , \*\*  $p < 0.01$ , ns denotes not significant. Since the regressions were statistically significant for AA and 1.5 x AA, we applied the ANCOVA; \*  $p < 0.05$ , ns denotes not significant.

1  
2  
3  
4  
5  
6  
7  
8  
9  
10  
11  
12  
13  
14  
15  
16  
17  
18  
19  
20  
21  
22  
23  
24  
25  
26  
27  
28  
29  
30  
31  
32  
33  
34  
35  
36  
37  
38  
39  
40  
41  
42  
43  
44  
45  
46  
47  
48  
49  
50  
51  
52  
53  
54  
55  
56  
57  
58  
59  
60  
61  
62  
63  
64  
65

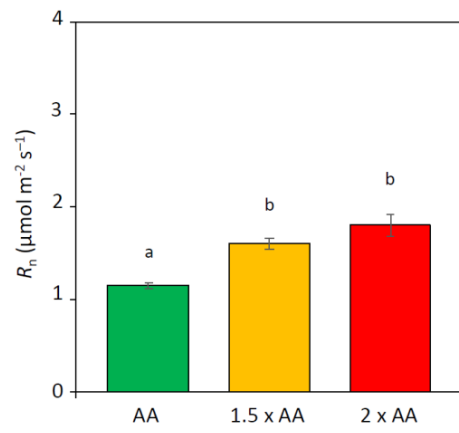


**Fig. 3** Average ( $\pm$  standard error) of dark respiration rate ( $R_n$ ) on July 30<sup>th</sup>. Different letters show significant effects of the ozone treatments (AA, ambient, 1.5 x AA, 2 x AA) (Tukey test,  $p < 0.05$ ,  $N = 3$  plots).

935

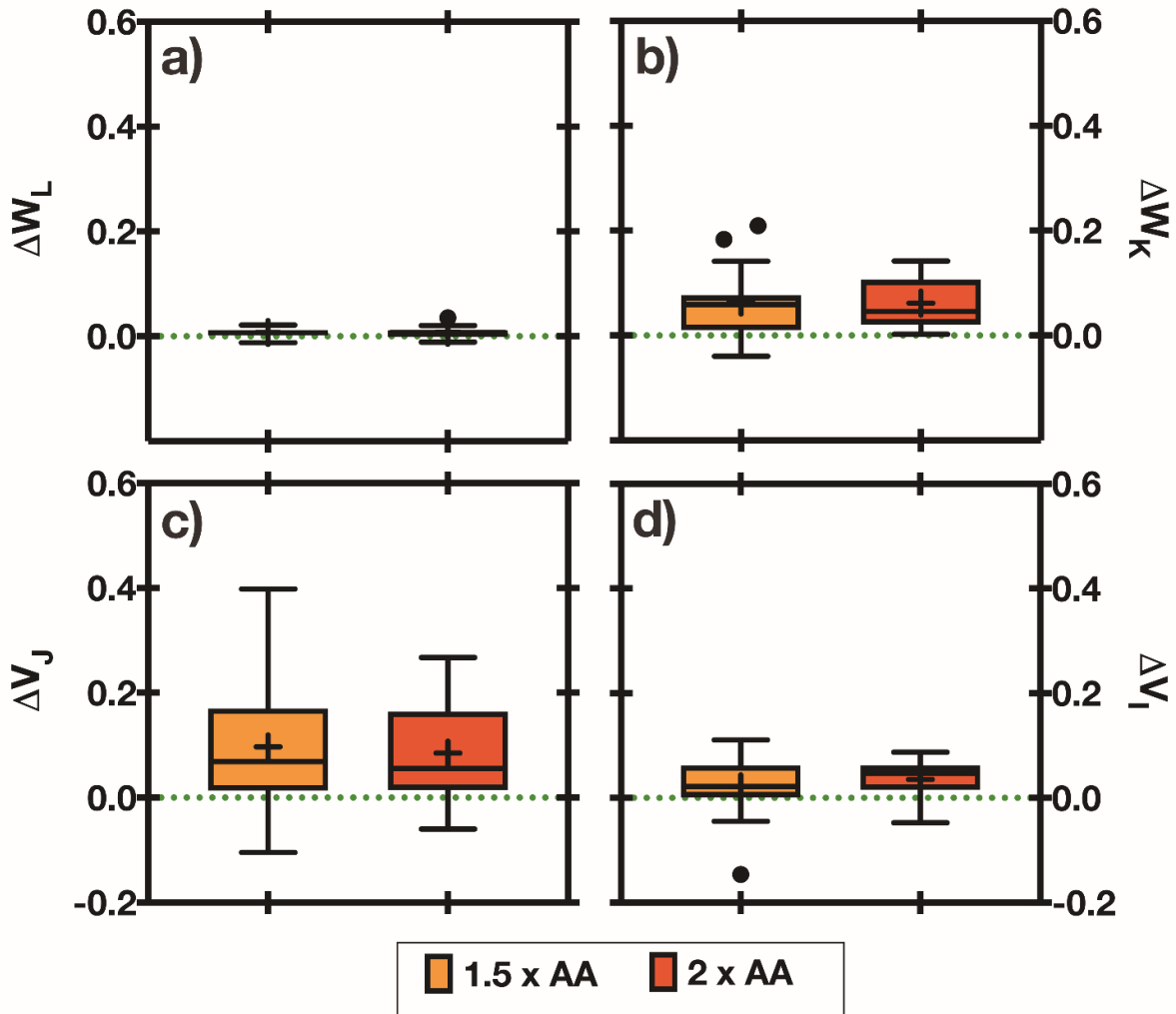


**Fig. 4.** Effect of different ozone levels on date palms, assessed with Chlorophyll-a fluorescence measurements *in vivo*. Boxplots show differences between elevated ozone levels compared to ambient ozone level (AA). Orange boxes, 1.5 x AA; red boxes, 2 x AA. Whiskers: 1,5 x IQR, dots: outliers, cross: average, line: median; green dotted line at  $y = 0$ : reference value at ambient ozone level;  $n = 3$  plots. (a)  $\Delta W_L$  difference of variable fluorescence  $\Delta W_{OK}$ , at the L-Step at  $t = 150 \mu s$ . (b) difference of variable fluorescence  $\Delta W_{OK}$ , at the K-Step  $t = 300-600 \mu s$ . (c) difference of variable fluorescence  $\Delta V$ , at the J-Step  $t = 2 ms$ . (d) difference of variable fluorescence  $\Delta V$ , at the I-Step  $t = 30 ms$ .



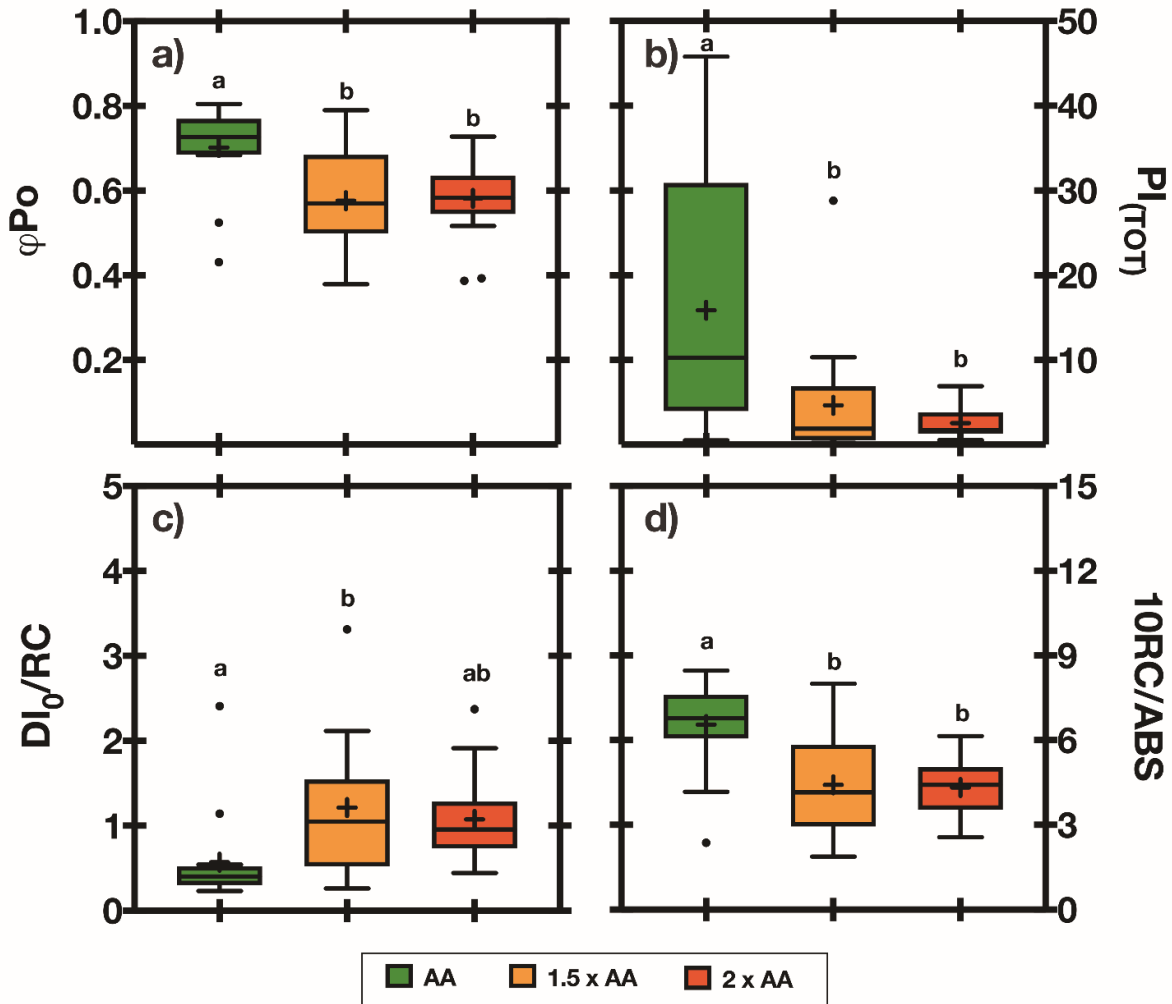


**Fig. 5.** Effect of different ozone levels on date palms on (a) maximum quantum yield for primary photochemistry  $\phi_{Po}$  (b) the performance index  $PI_{TOT}$ , (c) energy dissipation per active reaction centres  $DI_0/RC$ , (d) reaction centres per absorption  $10RC/ABS$ . Boxplots show: Green boxes, ambient ozone level (AA); orange boxes, 1.5 x AA; red boxes, 2 x AA. Whiskers: 1,5 x IQR, dots: outliers, cross: average, line: median. Different letters show significant differences among treatments (Tukey test,  $p < 0.05$ ,  $N = 3$  plots).

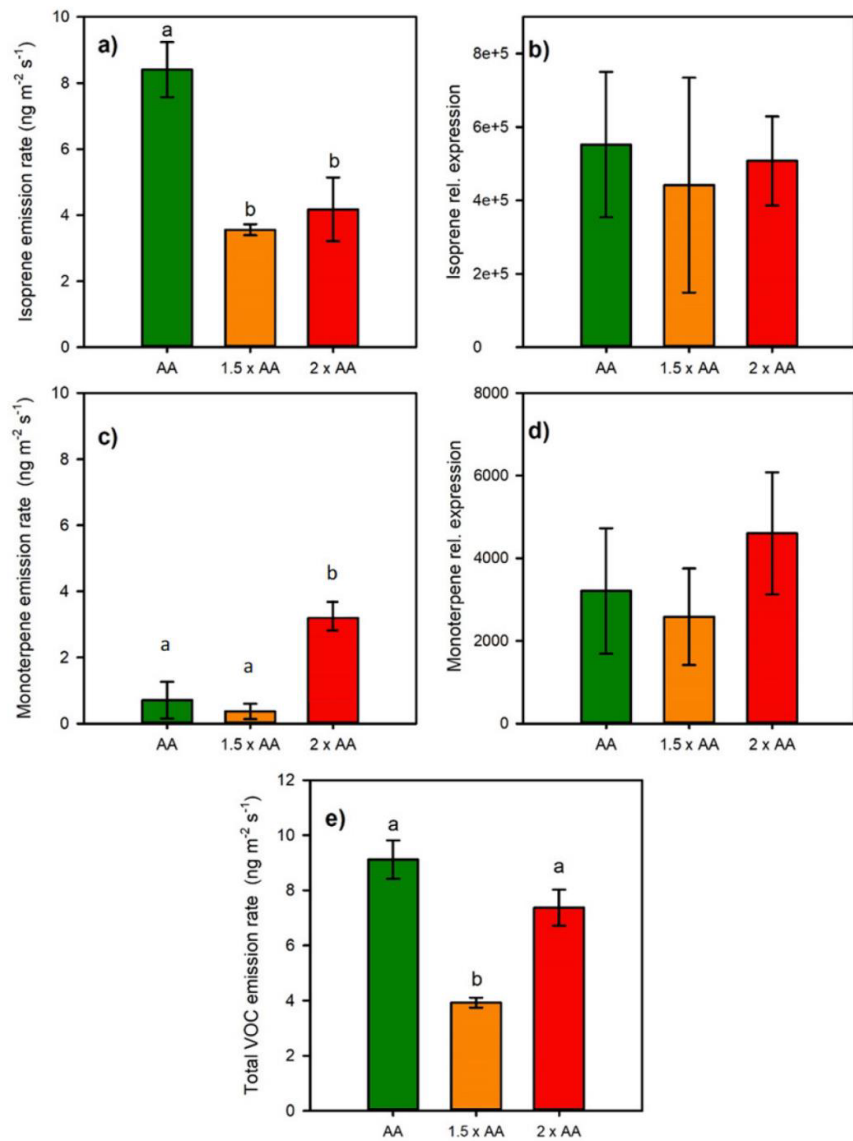


**Fig. 6** Average ( $\pm$  standard error) of isoprene emission (a), relative expression of isoprene synthase transcripts (b), monoterpene emission (c), relative expression of monoterpene synthases (d) and total volatile organic compounds (VOC) emission (e) in date palm leaves on 1-2 August. Different letters show significant effects of the ozone treatments (AA, ambient, 1.5 x AA, 2 x AA) (Tukey test,  $p < 0.05$ ,  $N = 3$  plots).

1  
2  
3  
4  
5  
6  
7  
8  
9  
10  
11  
12  
13  
14  
15  
16  
17  
18  
19  
20  
21  
22  
23  
24  
25  
26  
27  
28  
29  
30  
31  
32  
33  
34  
35  
36  
37  
38  
39  
40  
41  
42  
43  
44  
45  
46  
47  
48  
49  
50  
51  
52  
53  
54  
55  
56  
57  
58  
59  
60  
61  
62  
63  
64  
65

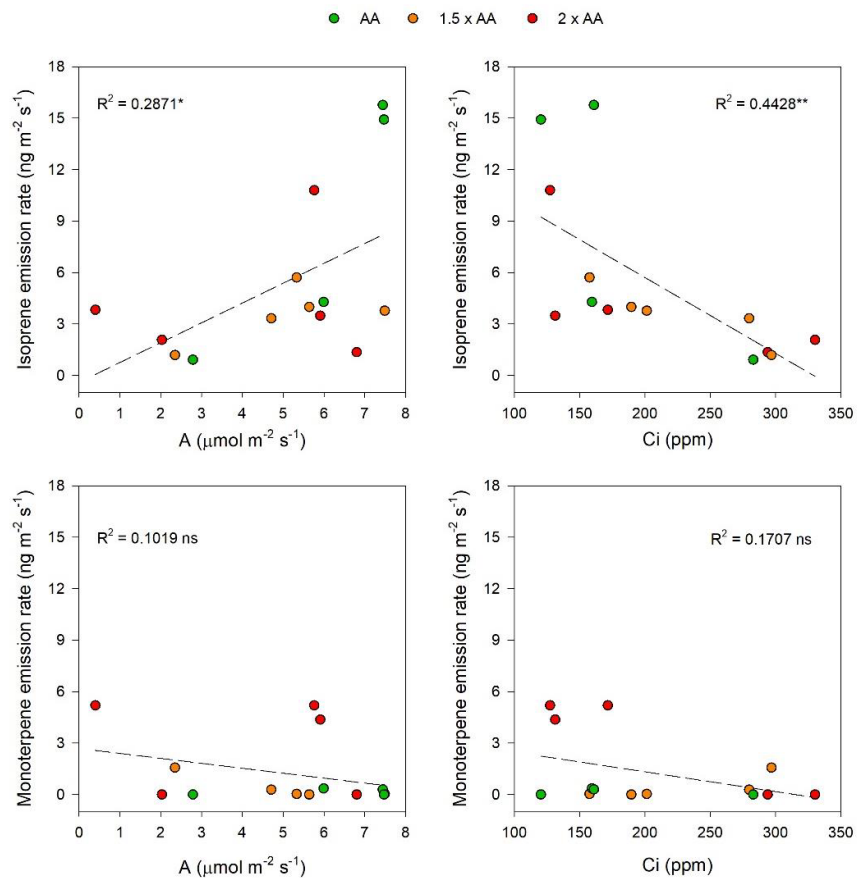


**Fig. 7** Relationships between BVOC emission and net photosynthesis (a, isoprene; c, monoterpene), intercellular CO<sub>2</sub> concentration (b, isoprene; d, monoterpene) in date palm leaves grown under different O<sub>3</sub> concentrations (AA, ambient, 1.5 x AA, 2 x AA). Simple linear regression analyses: \*\*  $p < 0.01$ , \*  $p < 0.05$ , ns denotes not significant.

965  
1  
966  
3  
4  
5  
6  
7  
8  
9  
10  
11  
12  
13  
14  
15  
16  
17  
18  
19  
20  
21  
22  
23  
967  
24  
25  
968  
26  
27  
969  
28  
29  
970  
30  
31  
32  
971  
33  
34  
972  
35  
36  
37  
38  
39  
40  
41  
42  
43  
44  
45  
46  
47  
48  
49  
50  
51  
52  
53  
54  
55  
56  
57  
58  
59  
60  
61  
62  
63  
64  
65

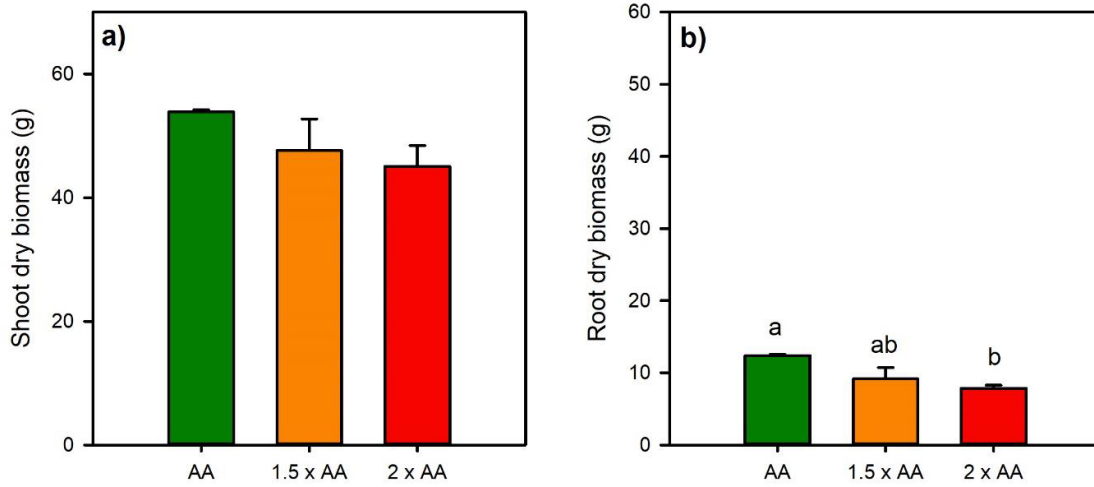


**Fig. 8** Above- (a) and below-ground (b) biomass of date palms on August 20<sup>th</sup>, i.e. at the end of 92 days of exposure to ambient ozone (AA), 1.5 x AA and 2 x AA. Different letters show significant differences among treatments (Tukey test,  $p < 0.05$ ,  $N = 3$  plots).

15  
16  
17  
18  
19  
20  
21  
22  
23  
24  
25  
26  
27  
28  
29  
30  
31  
32  
33  
34  
35  
36  
37  
38  
39  
40  
41  
42  
43  
44  
45  
46  
47  
48  
49  
50  
51  
52  
53  
54  
55  
56  
57  
58  
59  
60  
61  
62  
63  
64  
65

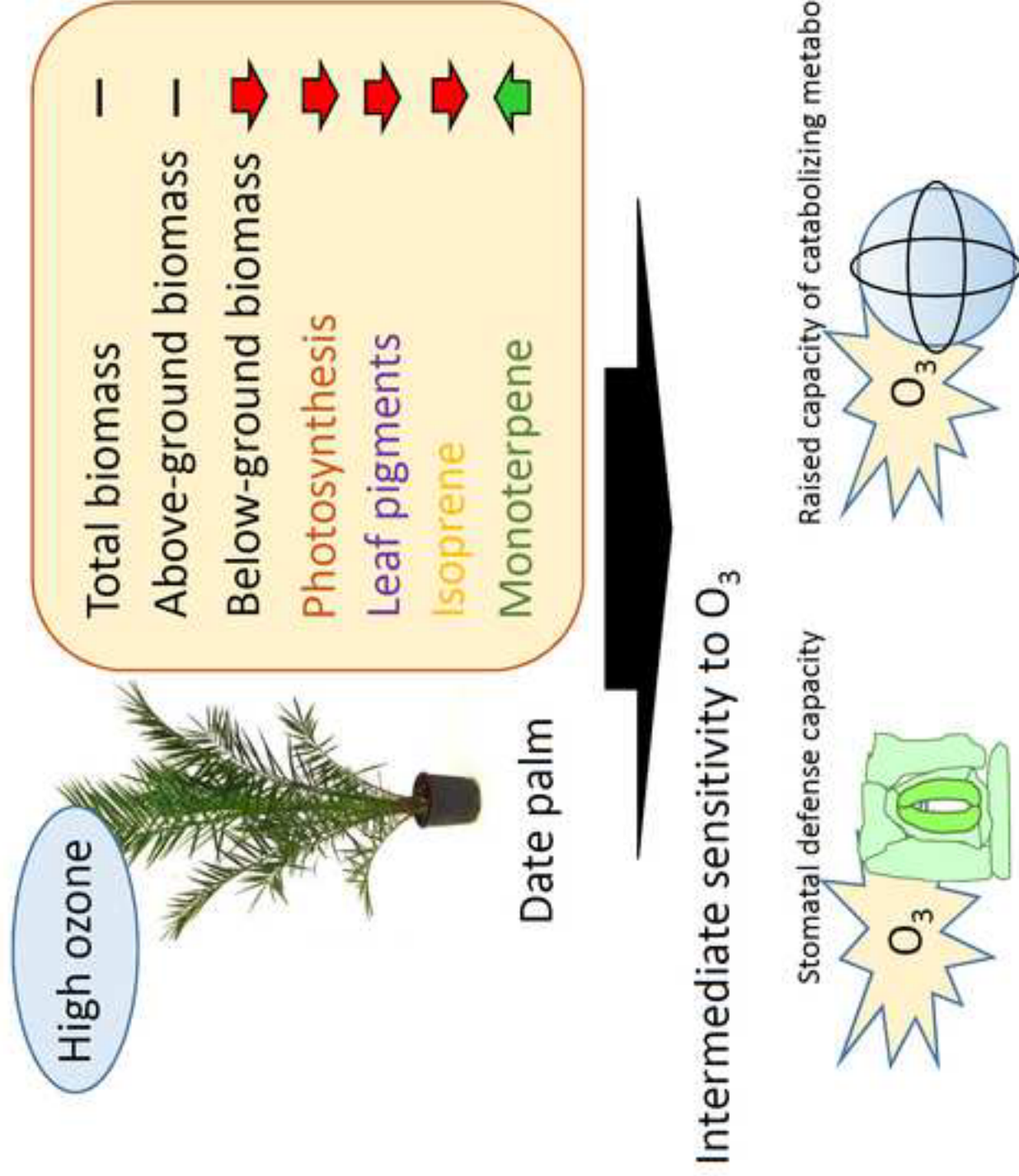
**Tab. 1.** Mass per area (LMA), water content (LWC), total chlorophyll content (Chl<sub>TOT</sub>), chlorophyll a/b ratio (Chl a/b), total carotenoid content (Car<sub>TOT</sub>), β-carotene (β-car), lutein (Lut), xanthophyll cycle pigment content (VAZ) and de-epoxidation state (DEPS) in the leaves of date palm plants grown under three levels of O<sub>3</sub> concentration (AA, ambient O<sub>3</sub> concentration, 1.5 × AA, 2 × AA). Each value is the mean ± standard error (N = 3 plots). Asterisks show the significance of ANOVA: \*\*  $p < 0.01$ , \*  $p < 0.05$ , ns denotes not significant. Different letters show significant differences among treatments ( $p < 0.05$ , Tukey test).

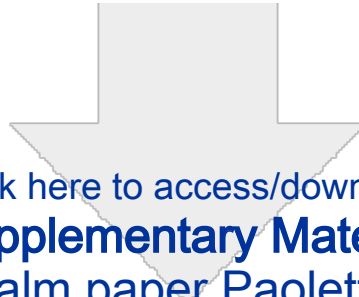
	LMA (g m <sup>-2</sup> )	LWC (%)	Chl <sub>TOT</sub> (μmol g <sup>-1</sup> FW)	Chl a/b	Car <sub>TOT</sub> (μmol g <sup>-1</sup> FW)	β-car (μmol g <sup>-1</sup> FW)	Lut (μmol g <sup>-1</sup> FW)	VAZ (μmol g <sup>-1</sup> FW)	DEPS (%)
AA	133.4 ± 9.8 a	45.8 ± 2.8 a	2.7 ± 0.1 a	3.5 ± 0.2 a	136 ± 8 a	2.1 ± 0.3 a	0.99 ± 0.02 ab	78 ± 3 a	46 ± 3 a
1.5 × AA	118.8 ± 3.3 a	52.2 ± 0.4 ab	2.1 ± 0.1 b	3.7 ± 0.1 a	92 ± 14 b	1.6 ± 0.1 a	0.82 ± 0.08 b	51 ± 9 b	52 ± 2 a
2 × AA	122.1 ± 4.8 a	54.5 ± 1.6 b	2.3 ± 0.3 ab	3.3 ± 0.1 a	114 ± 8 ab	1.8 ± 0.1 a	1.11 ± 0.09 a	60 ± 7 b	48 ± 7 a
<b>ANOVA results (p-values)</b>	<b>O<sub>3</sub> effect</b>	<b>O<sub>3</sub> effect</b>	<b>O<sub>3</sub> effect</b>	<b>O<sub>3</sub> effect</b>	<b>O<sub>3</sub> effect</b>	<b>O<sub>3</sub> effect</b>	<b>O<sub>3</sub> effect</b>	<b>O<sub>3</sub> effect</b>	<b>O<sub>3</sub> effect</b>
	0.329 ns	<b>0.040</b> *	<b>0.016</b> *	0.110 ns	<b>0.006</b> **	0.078 ns	<b>0.007</b> **	<b>0.007</b> **	0.335 ns

979 **Tab 2.** Average ( $\pm$  standard error) of the daily profiles of net photosynthesis (A) and stomatal conductance  
 980 ( $g_s$ ) of date palm leaves on July 23<sup>rd</sup> and 30<sup>th</sup> 2019. Asterisks show the significance of two-way ANOVA: \*\*  $p$   
 981  $< 0.01$ ; \*  $p < 0.05$ ; ns, not significant. Different capital letters show results of a one-way ANOVA with  
 982 daytime as a factor, while different lower-case letters show results of a one-way ANOVA with  $O_3$   
 983 treatments (AA, ambient, 1.5 x AA, 2 x AA) within each daytime as a factor (Tukey test,  $p < 0.05$ ,  $N = 3$  plots).

		A ( $\mu\text{mol m}^{-2} \text{s}^{-1}$ )	$g_s$ ( $\text{mol m}^{-2} \text{s}^{-1}$ )
July 23 <sup>rd</sup>	<b>Morning</b>		
	AA	6.3 $\pm$ 0.8 a	0.07 $\pm$ 0.01 a
	1.5 x AA	5.0 $\pm$ 0.3 ab A	0.06 $\pm$ 0.00 a A
	2 x AA	3.1 $\pm$ 0.3 b	0.03 $\pm$ 0.00 b
	<b>Afternoon</b>		
	AA	2.8 $\pm$ 0.4	0.04 $\pm$ 0.01
	1.5 x AA	2.6 $\pm$ 1.0 B	0.04 $\pm$ 0.01 B
	2 x AA	2.6 $\pm$ 0.4	0.04 $\pm$ 0.01
	<b>ANOVA results</b> ( <i>p-values</i> )	$O_3$ : 0.048 *	0.036 *
		Time: 0.001 **	0.041 *
	$O_3 \times \text{Time}$ : 0.081 ns	0.125 ns	
July 30 <sup>th</sup>	<b>Morning</b>		
	AA	7.4 $\pm$ 0.8 a	0.06 $\pm$ 0.01 a
	1.5 x AA	5.1 $\pm$ 0.7 ab A	0.05 $\pm$ 0.00 a A
	2 x AA	3.8 $\pm$ 0.5 b	0.03 $\pm$ 0.00 b
	<b>Afternoon</b>		
	AA	4.3 $\pm$ 1.2	0.04 $\pm$ 0.01
	1.5 x AA	3.9 $\pm$ 0.9 B	0.04 $\pm$ 0.01 A
	2 x AA	2.7 $\pm$ 0.2	0.03 $\pm$ 0.00
	<b>ANOVA results</b> ( <i>p-values</i> )	$O_3$ : 0.022 *	0.037 *
		Time: 0.016 *	0.248 ns
	$O_3 \times \text{Time}$ : 0.383 ns	0.206 ns	

Graphical abstract.tif

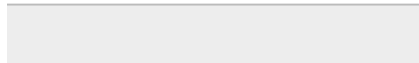
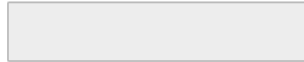




[Click here to access/download](#)

**Supplementary Material**

Supplementary Palm paper Paoletti et al.FINAL.docx





**Conflict of interest**

The authors declare that they have no conflicts of interest.

**Declaration of interests**

The authors declare that they have no known competing financial interests or personal relationships that could have appeared to influence the work reported in this paper.

The authors declare the following financial interests/personal relationships which may be considered as potential competing interests: